Super-resolution microscopy as a powerful tool to study complex synthetic materials

Super-resolution microscopy: a powerful tool to study complex synthetic materials

Silvia Pujals[1], Natalia Feiner-Gracia[1], Pietro Delcanale[1], Ilja Voets[2], Lorenzo Albertazzi[1,3]

[1]Institute for Bioengineering of Catalonia (IBEC), The Barcelona Institute of Science and Technology (BIST), Baldiri i Reixac 10-12, 08028 Barcelona, Spain

[2]Laboratory of Self-Organizing Soft Matter, Laboratory of Macromolecular and Organic Chemistry, Department of Chemical Engineering, Institute for Complex Molecular Systems (ICMS), Eindhoven University of Technology, 5612AZ Eindhoven, The Netherlands

[3]Department of Biomedical Engineering, Institute for Complex Molecular Systems (ICMS), Eindhoven University of Technology, 5612AZ Eindhoven, The Netherlands

ABSTRACT

Understanding the relations between the formation, structure, dynamics and functionality of complex synthetic materials is one of the great challenges of chemistry and nanotechnology and represents the foundation for the rational design of novel materials for a variety of applications. Initially conceived to study biology below the diffraction limit, super-resolution microscopy (SRM) is emerging as a powerful tool to study synthetic materials due to its nanometric resolution, multicolor ability and minimal invasiveness. In this Review, we provide an overview of the pioneering studies that use SRM to visualize materials, highlighting the exciting recent developments such as experiments in operando wherein materials are imaged in action, such as biomaterials in a biological environment. Moreover, the potential and the challenges of the different SRM methods for application in nanotechnology and (bio)material science are discussed aiming to guide researchers to select the best SRM approach for their specific purpose.

[H1] INTRODUCTION

Super-resolution optical microscopy has been recently introduced and rapidly revolutionized the way we look at biological systems, allowing us to visualize cell structures with unprecedented resolution. According to Abbe's criteria, the spatial resolution of fluorescence microscopy (FM) is limited by light diffraction to a few hundreds of nanometers, hampering the imaging of molecular structures on smaller length scales. Super resolution microscopy (SRM), or nanoscopy, has recently surfaced as a powerful technique to complement and overcome the current limitation of existing imaging approaches [1,2]. The SRM family encompasses a range of far-field optical techniques that exploit a number of chemical and physical principles to overcome the diffraction limit and enable nanometric-resolved imaging. The impact of SRM has been acknowledged with the Nobel Prize for Chemistry in 2014 [3].

Recently, SRM technologies have become influential in chemistry and material science as a mean to unveil the structure and dynamics of complex materials and materials. Importantly, the minimal invasiveness of optical microscopy facilitates visualization of materials in situ and in operando, for example in living cells or during catalytic processe. Therefore, the use of SRM is increasing in numerous fields including supramolecular chemistry, plasmonics, catalysis and biomaterials, complementing existing techniques such as atomic force microscopy (AFM) [4], electron microscopy (EM) [5], ensemble scattering methods and optical spectroscopy.

Our review highlights the advances in the application of SRM to the study of synthetic materials with a focus on biomaterials, and describes the more broadly the perspectives of these techniques in chemistry.

[H2] Why super resolution for synthetic materials?

Understanding the structure and the functionality of synthetic materials is critical for the development of improved materials for a variety of applications[6]. This is even more crucial in the case of complex molecular systems, as their dimensions, modular composition, hierarchical structure, and dynamics pose a serious challenge for their study with spectroscopic and microscopic techniques like AFM[7], EM[8] and FM[9]. The use of multiple complementary techniques is highly recommended as each method has its advantages and limitations related to operational requirements and contrast. AFM and EM, for example, offer excellent spatial resolution and do not require any labeling but their required invasive sample preparations, that usually involve freezing or drying procedures, that hamper imaging in native conditions. Furthermore, both techniques have limited permeation through the sample, usually confined to material surfaces or thin sections, and do not enable multicolor imaging making difficult or even impossible the identification of different molecular species in the sample. On the contrary, fluorescence microscopy enables the multicolor imaging of materials in native conditions as well as in biological environment, at the cost of limited spatial resolution. SRM overcomes this limit and allows us to access information on the nanometric scale without the need of invasive sample preparations. The three main types of super resolution methods are structured illumination microscopy (SIM), stimulated emission depletion (STED) and single molecule localization microscopy (SMLM) (Box 1). These three approaches are characteried by different and often complementary features, thus a critical step is the choice of the ideal techniques for the scientific question of interest.

The appeal of SRM to study complex synthetic materials is manifold. First, the nanometric spatial resolution down to 5 nm allows us to resolve 3D molecular structures and link them with the functionality they are responsible for. Synthetic molecular architectures are often hierarchical structures with a defined order on different length scales. Nanoscopy can resolve such multi-scale structural features with nanometric accuracy as an image can cove a rather large field of view (for example, 100µm x 100µm).[10] Another intrinsic characteristic accessible by nanoscopy

is the complex composition of advanced materials. The multiple building blocks that are incorporated in a material in a modular fashion (for example, multiple functionalities on the same scaffold) can be uniquely identified in space as a function of time. Typically, three different sets of molecules can be separately labeled and imaged, however, examples of 6-color [11] and 10-color imaging[12] have been proposed using SMLM. The multicolor quantitative nature of SMLM allows us to visualize and count different molecules, therefore providing information on the stoichiometry of synthetic assemblies[13]. The development of approaches to simulate SMLM images can greatly help the interpretation of quantitative SMLM analysis [14]. Another interesting aspect of complex materials is related to their ability to continuously change structure over time. This is particularly relevant for supramolecular structures, materials based on dynamic covalent chemistry and out-of-equilibrium materials. The dynamic nature of these materials is responsible for some of their most intriguing properties such as responsivity, adaptivity and self-healing. Understanding of such molecular dynamics is as much important as challenging, due to the multiple time and spatial scales involved in this phenomenon. Finally, it is very important that any characterization technique should probe the system of interest in the closest conditions to the real operational environment of the material. Often spectroscopic and microscopic analysis are usually performed in idealistic conditions (such as, pure water) that are poorly representative of the real world (for example, a living cell, the complex matrix of a material, a complicated device). SRM, thanks to its minimal invasiveness, multicolor imaging ability and temporal resolution, is an ideal technique to prove and unveil molecular structure and dynamics in situ (Box 2).

In this review we will discuss the most relevant works using SRM to study various classes of synthetic materials including supramolecular fibers, polymer-based materials, lipid-based materials, DNA origami and metal nanoparticles. Moreover, the imaging of materials in situ, i.e. in their operational conditions will be analyzed. Electronic devices and catalytic devices have been extensivecly reviewed elsewhere[15,16], while this review will focus on the use of super-resolution to image biomaterials in the biological environment. Altogether this review will provide a comprehensive picture of the use of super-resolution imaging in the chemistry field and offer a guide towards the choice of the proper imaging methods to address a scientific question in the material arena.

[H1] SRM for molecular observations in vitro

In this section, we review the most relevant contributions to the development of SRM for the study of complex molecular architectures. Several families of materials have been studied demonstrating the generality of nanoscopy to image virtually any chemical structure.

[H2] Supramolecular polymers and nanofibers

Supramolecular polymers are polymers in which the monomers are linked by non-covalent bonds, typically by hydrophobic interactions and hydrogen bonding. Their dynamic nature together with their modularity and responsiveness to different stimuli makes them promising candidates for several applications in biomedicine, optoelectronics, sensing and catalysis[17]. SRM proved in the last years to be a powerful method to study the structure and dynamics of supramolecular polymers, providing complementary information to those attained with ensemble techniques (UV spectroscopy, circular dichroism, X-ray scattering) and label-free imaging techniques (EM, AFM).

Albertazzi & Meijer reported the first example of supramolecular polymer imaging using SRM[18]. They investigated the monomer exchange mechanism of water-soluble 1,3,5-benzenetricarboxamide (BTA) supramolecular polymers using a particular SMLM approach known as stochastic optical reconstruction microscopy (STORM). The study reported on a 2-color STORM method to achieve dynamic information —such as the exchange of monomers between fibres — using a static technique. This is possible by labelling two batches of materials with two spectrally-distinct dyes and following green-labeled monomers joining red-labled fibres and vice versa at specific time-points, so that temporal information are imprinted into spectral information. Before the use of SMLM, monomer exchange along a fibre was usually explained by polymerization/depolymerisation occurring at the end of fibers or by a fragmentation/recombination mechanism based on data acquired from ensemble studies, i.e. a study of the bulk solution. However, the combination of STORM and stochastic modelling demonstrated that a homogeneous exchange occurs all along the BTA self-assembled fibrillar structures. This study was followed by several other reports on the use of the 2-color STORM method. In particular, these studies unveiled how the dynamics of supramolecular polymers is influenced by hydrophobicity and chirality[19] and by the presence of functional groups[20]. Notably, tracking and locating specific monomers in a mixture of different components can be performed only thanks to the combination of nanometric resolution and specific labelling. The studies mentioned above were performed in water to explore the potential use of BTA polymers for biomedical applications. However, methods that enable super resolution imaging of supramolecular structures, such as, BTA fibres in methyl cyclohexane in organic media have also been developed [21–23]

In addition to BTAs, other families of supramolecular polymers have been studied using nanoscopy, including ureidopyrimidinone (Upy)-based polymers and peptide amphiphiles[24]. In both cases the mechanism as well as the kinetics of monomer exchange was unveiled and the structure–dynamics relationships highlighted. Altogether, these nanoscopy studies highlight that the dynamic properties of a polymer material depend on how ordered the assemblies are. Ordered structures are more static than disordered ones in which structural defects introduce exchange points that make the materials more dynamic. Static and dynamic structures can

co-exist as is the case of peptide amphiphiles, in which fully dynamic areas coexist with kinetically inactive areas within the same fibril[25]. Building upon previous work that enabled photo-activation localization microscopy (PALM) in organic solvents[21] and interface point accumulation for imaging in nanoscale topography (iPAINT) in aqueous media[26], the internal block-like arrangement of dissimilar monomers within supramolecular nanowires was elucidated by 2-colour imaging in organic solvents using iPAINT[23]. The quasi-permanent adsorption of both dyes by the polymer in methylcyclohexane was exploited to identify the blocks within the supramolecular fibers, which were prepared by mixing pre-stained homopolymers. The combination of SRM and spectroscopy holds great promise to study the photophysical properties of intrinsically fluorescent nanofibers. Scheblykin and coworkers[27] exploited the blinking behavior of perylene bisimide supramolecular polymers to map spatially and temporally the energy transfer along fibrillar aggregates. This paves the way towards the use of nanoscopy to unveil the properties of supramolecular materials with relevant applications in energy and electronics.

Among self-assembled materials, small molecular hydrogelators are commonly used for tissue engineering because they are easily prepared, inexpensive and exhibit interesting properties (such as, self-healing). An exciting possibility is represented by double-network hydrogels obtained by the mixing of two orthogonal hydrogelators that self-sort, i.e. assemble in independent structures, into an intermixed structure. However, the self-sorting (and not the co-assembly- a structure formed by two individual components-) of the two building blocks cannot be easily elucidated by means of techniques including, solid-state NMR, fluorescence spectroscopy, SAXS, TEM, SEM, AFM, as these do not allow us to follow two separate molecules in-situ inside a 3D gel structure. Recently, the Hamachi's group has observed self-sorting in supramolecular fibers using confocal laser scanning microscopy (CLSM) and STED imaging[28] (FIG. 2a). The group used two types of hydrogelators — one peptide-based and one lipid-based with cationic, zwitterionic or anionic head groups — labelled with two spectrally-separated dyes. Self-sorting was visible by CLSM, but was clearly better visualised by higher resolution STED (Fig. 2b), as the fibre diameter was below the resolution limit (80-100 nm). STED-based colocalization unambiguously indicated that there was a weak correlation between the two-channels, confirming the self-sorting of the two-fiber network. STED, due to its ability to image through a thick sample, is the ideal technique to image hydrogelators and might be a powerful tool for the investigation of supramolecular scaffolds for tissue engineering.

Altogether, nanoscopy has demonstrated to be a powerful tool for the characterization of supramolecular fibres. SRM added the multicolour dimension to the imaging of these structures, typically imaged with AFM and EM, allowing us to perform nanometric colocalization between different structures and monomers and to follow the fate of individual molecular species into a multicomponent material. Recently, SUSHI (Super-resolution SHadow Imaging) method, based on 3D-STED and the use of diffusible fluorophores in order to image large fields of view without photobleaching nor phototoxicity, has been used to study biological tissues

like the extracellular matrix[29]. It could be a source of inspiration to further study the complex 3D morphology of supramolecular fibres and hydrogels.

[H2] Polymer-based materials

The pivotal role of polymers in material science originates from their unique structure–property relations. SRM has offered new insight into structural features such as (micro)phase separation, association states, and morphologies that are often critical for the optimal performance of a polymer material. For example, the photophysical properties of conjugated polymers in light emitting diodes and organic solar cells are dependent on the conformation of the individual macromolecular chains and their organization into microdomains, thus directly impacting the efficiency of the devices. Due to the large variety of obtainable structures, such as micelles, vesicles and fibers (Fig. 3a),[30] block copolymers are probably the family of materials for which the widest range of nanoscopy methods have been used (STORM, PALM, STED, isoSTED, SIM) and represent a good example of how to choose the best technique in view of the structural and functional features of the target materials. Manners and coworkers observed for the first time block copolymers forming fiber-like structures[22] and rectangular platelet micelles[31] using SIM, STED and PALM (FIG. 3b). Remarkably, SIM does not require the aid of any special dye and provides good time resolution enabling ease of sample preparation and time-resolved studies , for example, of the kinetics of fiber formation in organic solvents [22]. This study demonstrates the power of SRM not only to attain high resolution images but also to gain molecular information from the measurements of polymeric structures of a large variety of sizes and shapes.[31] Analogously to supramolecular polymers the 2-color modality of SRM was used to observe phase-separation or colocalization of different molecular species in the materials. IsoSTED has also been used to study the 3D structure of poly(styrene-*block*-2-vinylpyridine) (PS-*b*-P2VP) block copolymer films.[32] This method relies on a combination of a STED and a 4Pi microscopy that allows us to noninvasively and rapidly image nanoscale morphologies spanning the whole volume of the sample. The ability to image in 3D large samples is crucial for the understanding of complex materials exhibiting hierarchical morphologies.

Imaging morphological changes in block-copolymer assemblies is of great interest for the development of responsive materials. As a relevant example, Yan et al. imaged the transition from cylindrical micelles to polymersomes of poly(styrene-*block*-ethylene oxide) (PSt-*b*-PEO)[33]. To this end, spiropyrans were incorporated in the hydrophobic, glassy-like poly(styrene) core of the PSt-*b*-PEO micelle formed in water. Profiting from the stochastic blinking of spiropyrans in hydrophobic, solid-like environments, the spiropyran-containing microphases were readily imaged yielding reconstructions of both the cores of cylindrical micelles and the bilayer walls of the polymersomes with nanometer resolution.[33]

Protein polymers represent an interesting family of semi-synthetic materials that exploit the programmability and biocompatibility of recombinant proteins. Polyaminoacids composed of hydrophobic and hydrophilic blocks have been proposed and tested for biomedical applications.[34] Beun et al. used STORM to investigate whether both

ends of µm-long protein–polymer nanofibres are living (that is, are not terminated) once polymerization has ceased and whether growth proceeds in one or two directions (for example, from one or both fiber ends) .[35] First, a well-known fiber forming triblock protein-polymer was selected, that comprises a self-assembling silk-like domain and features two water-soluble collagen-like domains at both ends. Next, nanofibers were formed in aqueous solutions of triblocks bearing Alexa-647 (red). Time-lapse SRM imaging on thus synthetized protein-polymer nanofibers revealed that added Alexa-488 (green) labeled triblock protein-polymersattach to only one of the two fiber ends, resulting in the formation of green-red diblock fibers, indicating uni-directional growth.

Complex coacervate core micelles (C3Ms), also known as polyion complex micelles, are a novel class of association colloids composed of polyelectrolytes. Their assembly is electrostatically driven rather than hydrophobically as for amphiphilic polymers. Aloi et al. used iPAINT to visualize the concentration-induced shape evolution of C3Ms composed of polyfluorene and poly(N-methyl-2-vinyl pyridinium chloride)-*b*-poly(ethylene oxide.[26] Moreover, Vicent and co-workers measured size, shape and the dynamic exchange of polymers between aggregates of charged polymers using 2-color STORM.[36] In this case, the self-assembly induced by the attraction of polyions at low salt content was monitored by a combination of STORM and a variety of other spectroscopy and microscopy techniques that unequivocally provided the first experimental evidences of the theoretically predicted 'extraordinary' charge-driven aggregation mechanism. Although only a few studies of coacervates using SRM have been reported so far, they highlight that optical imaging is a potentially powerful tool to visualize and probe properties of soft materials that are difficult to study with other approaches. An interesting future perspective is to exploit SRM to address the molecular composition and stoichiometry of the two charged species with single aggregate resolution. The conformation of individual conjugated and non-conjugated macromolecular chains in polymer blends has been captured successfully by SMLM.[37,38] Aoki et al. used PALM to visualize the architecture of poly(butyl methacrylate) (PBMA) labeled with rhodamine spiroamides and embedded in a thin film of unlabeled PBMA spincast on a glass cover slip.[39] Gramlich et al. used STORM to image the nanoscale morphology of polystyrene and polymethyl methacrylate blends.[40] The group determined size, shape and abundance of demixed nanodomains in the thin films and found a correlation between these characteristics and film thickness. Not only the inner structure, but also the surface properties of polymer materials can be investigated with nanoscopy. Indeed, STORM experiments revealed the surface densities and heterogeneous distributions of dye-labeled −COOH groups on different poly(methyl methacrylate) surfaces.[41]

The intrinsic fluorescence of conjugated polymers is typically emitted from localized regions within individual chains. The migration of excitons and its dependence on the polymer conformation are critical, yet partially understood, parameters for the performances of such polymers in optoelectronics (such as light emitting diodes, solar cells), as (force) sensors and as fluorescence markers.[15,38,42] Offering unprecedented access to both the single-chain conformation and exciton density, SRM can play a pivotal role in unravelling the link between the structure and photophysical properties of conjugated polymers. Habuchi and co-workers

exploited the blinking of individual poly[2-methoxy-5-(20-ethylhexyloxy)-1,4-phenylene vinylene] (MEH-PPV) chains embedded in thin films of Zeonex or polystyrene[43] to map the emitting sites within individual chains. The label-free SMLM experiments revealed both the MEH-PPV architecture (rod-like or disc-like) and the density of emitting sites, which were approximately 10 nm apart and distributed in a uniformly manner.[44] Similarly, Park et al. resolved closely spaced emission sites after stepwise photobleaching of single emitters using the so-called single-molecule high-resolution imaging with photobleaching (SHRImP).[45] Penwell et al. resolved structural features down to 90 nm of poly(2,5-di(hexyloxy)cyanoterephthalylidene)-based nanoparticles that carried densely packed endogenous chromophores employing a modified STED scheme that featured an excitation laser modulation.[46] King and Granick imaged operating organic light-emitting diodes composed of MEH-PPV. They used STED-spectral imaging to map the conformation of the chains in the emissive layer, and electroluminescence-STED (EL-STED) to obtain super-resolved (~50 nm resolution) electroluminescence maps along the axial direction and in *x*–*y* plane.[47] These examples beautifully illustrate how well suited SMLM is to disclose the structure–function relations of this special class of polymers. Their intrinsic fluorescent blinking enables a label-free single-molecule reconstruction of their chain conformation and a direct assessment of the spatial distribution of their functional sites. Accessing this information will help us further understand the physical underpinnings of the performance of conjugated polymers in molecular electronics applications.

Widely used fluorescent dyes for SRM are often suboptimal for the visualization of polymer materials due to latter's size, hydrophobicity and limited exposure to solvent. The first generation of nanoscopy labels for biological structures were designed to covalently bind the hydrophilic surface of proteins. The steadily increasing interest in SRM from the polymer and materials science communities has catalyzed the development of novel dyes tailored for nanoscopy in complex environments like solvent-free polymer blends and hydrophobic cores of block copolymer micelles. [48–51] Moreover, one of the main limitations of STORM is the necessity of adding cofactors to the solvent to achieve the desired photoswitching. To overcome this limitation, several groups have proposed alternative dyes for super resolution imaging that spontaneously photoswitch and can be incorporated into block copolymers. Tian, Li and Hu proposed[48] the use of spiropyran derivates to perform single molecule localization microscopy (PULSAR) and reconstructed images with a resolution down to 10-40 nm[52] at the cost of long exposure times (1s) and poor temporal resolution. Similarly, Yan and coworkers explored the possibility to use spiropyran derivates dyes to image block copolymers (PSt-*b*-PEO) self-assembled into cylindrical micelles in aqueous media.[50] A diarylethene derivative has been investigated by Nevskyi et. al.[51] as a novel photoswitch for PALM imaging due to its high photostability and strong fluorescence of one of its conformations. As in the case of spiropyran derivates dyes, two laser wavelengths are used to convert the diarylethene dye from the non-fluorescent to the fluorescent form and vice versa. The authors demonstrated the possibility to visualize micelles assembled from PSt-*b*-PEO block copolymers with SMLM.

Although polymers are usually fluorescently labeled in order to be studies with SRM, some polymers may exhibit intrinsic fluorescence in the visible range.[53] PMMA, polystyrene and Su-8 films were imaged using STORM without any external labelling showing intensive blinking events that enabled the reconstruction of a well-defined image. [53] The intrinsic fluorescent properties of several materials represent at the same time an advantage and a drawback as the spontaneous fluorescence generates a strong background that prevents high resolution visualization of the structure through specific labeling. Therefore, the development of novel blinking dyes that are emissive in the polymeric environment and the development of self-blinking materials suitable for label-free SMLM represent two interesting perspectives in SRM.

[H2] Lipid-based materials

Liposomes and lipid nanoparticles play a crucial role in a wide range of biomedical applications such as drug delivery[54]. The typical liposome size range from 50 nm to 200 nm can be addressed perfectly by SRM. The hydrophobic nature of the bilayer interior of liposomes makes these assemblies ideally suited for PAINT using lipophilic probes. The first examples of PAINT involved the use of hydrophobic probe Nile Red to image 100 nm diameter large unilamellar vesicles (LUVs) and a supported lipid bilayer (SLB)[55] (Figure 4a). Nile Red is an ideal probe in PAINT, because its fluorescence emission is almost negligible in water but strong in apolar environments. Moreover, the Nile Red association time to lipids of around 6 ms is suitable for on/off switching, thus enabling single molecule localization[55]. In later studies, PAINT was exploited to visualize the lateral phase separation of distinct lipids that resulted in the formation of small domains within membranes. This phase separation remains challenging to image with other techniques[56]. Spectrally-resolved PAINT (sPAINT) has also been introduced[57,58] (FIG. 4b): Sharonov et al. exploited the environment-dependent emission of the Nile Red to map the hydrophobicity of the structures, providing an extra dimension to the super resolution image. The insertion of a transmission diffraction grating into the optical path enables the acquisition of fluorescence spectra of individual solvatochromic fluorophores and leads to high-resolution maps of the hydrophobicity of LUVs and other structures, such as β-amyloid(1-42) fibers, α-synuclein fibrils and the cell plasma membrane. This pioneering example highlights how SRM can not only reveal structural information, but also probe the chemical properties of supramolecular biomaterials.

In addition to the characterization of morphology and size, insight on the internal structure of micelles and vesicles provides valuable information. A first quantitative study to assess encapsulation and compartmentalization in nanostructured lipid carriers (NLC) was performed by Boreham et al. [59]. They combined STORM imaging and single-particle tracking approaches to measure the size and shape of the NLC domains loaded with ATTO-Oxa12 fluorescent dyes with 6 nm spatial resolution. This approach allowed the group to monitor the precise distribution of drugs inside the NLCs, revealing the existence of two types of drug-loaded nanocompartments of different size (Ø ~70 nm and 120-130 nm) that fill up to ~50% of NLCs' volume.

More recently, attention has been dedicated to the study of lipid nanoparticles and their surface functionalization, which can be considered one of the major mechanism of nanoparticle–cell interaction. In a recent report Van Oijen and coworkers[60] reported the molecular counting of functional proteins on the surface of liposomes using single molecule imaging. This study opened the way toward multicolor mapping of the functionality of lipid-based drug nanocarriers.

The unique characteristics of liposomes bring with them both advantages and disadvantages for SRM studies. Although the hydrophobicity of the intramembrane compartment enables PAINT with polarity probes, difficulties in fixation and lack of stability of lipid assemblies challenge other methods such as STORM or STED. The development of novel sample labeling and preparation procedures will open new avenues in liposomes nanoscopy imaging.

[H2] DNA origami

Among nanostructured materials, DNA origami[61] gained a prominent position due to versatility and high programmability of the DNA assembly [62]. However, their small size and complexity makes DNA origami rather challenging to be characterized with nanoscale accuracy; for this reason, super-resolution imaging of DNA origami is gaining growing attention since the first reports of such materials [63].

Tinnefeld and coworkers have been among the firsts to use STORM to image DNA origami. They were able to visualize and measure with nanometric resolution the distance between two labeled strands that populated the diagonally opposite corners of a rectangular DNA assembly of known dimensions [64]. STORM measurement of the labeled strands (88 nm) resulted in excellent agreement with the designed diagonal length (89.5 nm). This pioneering work demonstrated that SMLM is an effective tool to study DNA origami and that DNA origami can be used as calibration standard for SRM. Indeed, the controllable design of DNA origami at the molecular level enables the creation of nanorulers to test the performances of a specific SRM setup. For this purpose DNA origami decorated with fluorophores at nanometric distances have been designed and used to challenge STED, SMLM and SIM microscopy[65,66]. The same group extended the use of dSTORM to attain 3D images of DNA origami, as in the case of DNA- nanopillars, demonstrating the ability of this technique to resolve both origami structure and orientation[65].

Being composed by DNA strands, origamis are considered ideal structures to be studied with DNA-PAINT, as shown by Jungmann, Simmel and coworkers [67] . Extra oligo sequences acting as docking strands can be included in the origami structures, while complementary dye-labeled sequences are added to the solution as imager strands (Fig. 5a). Several origami structures have been imaged using DNA-PAINT and a particular elegant example is the DNA rigid closed hollow tetrahedron structure featuring 75 nm sized edges [68]. Authors succeed in binding fluorescent molecules at the edges of a tetrahedron, thus validating its potential as 3D ruler for SRM ~~(FIG. 2d)~~.

DNA-PAINT was also used to look at structure and orientation of single-stranded tiles (SSTs) that featured labeled docking strands at the four corners. Simmel and coworkers succeeded in imaging with DNA-PAINT [69] one of the smallest DNA structures: a scaffold-free DNA cube, the edges of which are 32 base-pairs long. DNA-PAINT has also been used to identify gene sequences by means of relatively inexpensive short ssDNAs with a sequence resolution of 50 nucleotides that corresponds to a spatial resolution of 30 nm.[70] Knudsen and co-workers studied the immobilization of polymers into a DNA origami structure by DNA-PAINT[71], as a first step towards the creation of hybrid origami-polymers biomaterials.

Other implementations of DNA-PAINT have been developed with the aim of reducing the image acquisition time and the background level. Schueder and coworkers achieved a faster and less invasive DNA-PAINT imaging of 3D DNA origami using a spinning disk microscope [72]. A fluorescence resonance energy transfer (FRET)-based version of DNA-PAINT was interestingly developed by Auer et al., who introduced specific single strand docking sequences of programmable length to a DNA origami scaffold. In this approach, the single molecule localizations are related to a FRET event so that backgroundlevel and image acquisition time of DNA-PAINT are significantly reduced[73]. Additionally, counting of densely packed organic fluorophores was demonstrated by analysis of their photo-switching kinetics during STORM imaging. In this case, a DNA-origami scaffold was decorated with two trimers of closely packed organic fluorophores, that are not individually resolvable with STORM but can be discriminated by means of the image analysis[74]. STED microscopy has been also used to study the photophysical behavior of different fluorescent probes on DNA origami structures [75].

The relationship between DNA origami and nanoscopy leads to a clear mutual benefit. On one side, DNA origami are a promising new class of materials with complex features that need SRM as a powerful characterization technique. On the other, DNA origami are molecularly controlled scaffolds that can serve as a benchmark for super-resolution methods and labels, contributing to the advancement of the technique. For example, the use of DNA-PAINT for the study of DNA origami resulted in some of the best advanced performances currently reported in terms of multiplexing (up to 10 colors have been recorded [12]) 3D imaging[71,72] and resolution (being able to solve densely packed triangular lattice with 5 nm point to point distance with three different colors in multiplexed exchange-PAINT [12,76]).

[H2] Nanoparticles

The power of SRM to resolve subdiffraction structural and functional details of nanoparticles that are often much smaller in size than the diffraction limit is becoming increasingly recognized. Pioneering studies in this area have demonstrated the visualization of the morphology and surface functionalization of individual nanoparticles[21,26,77], their dense packing in clusters and colloidal crystals,[21,78] the plasmonic properties of

metallic nanoparticles and the catalytic properties of oxides. Nanoparticles can also facilitate SRM imaging of other materials, because they can serve as sensitive markers for drift correction to enhance precise localization and overlay, for example in correlative SRM and AFM/EM studies[79]. Bon et al. used dSTORM to localize gold nanoparticles in 3D space with nanometric accuracies down to 0.7 nm in the lateral and 2.7 nm in axial directions by collecting 50 frames per second, even in the presence of micron-large fluctuations[80].

Large, micron-sized colloids have long been studied using scattering methods and quantitative confocal imaging as experimentally accessible model systems for atoms. The advent of SRM offers the possibility to access time-lapse real-space information on the phase behavior and superstructure formation in the entire colloidal space domain (nm–µm). For example, Harke et al. used 3D STED imaging (with a lateral resolution of 43 nm and an axial resolution of 125 nm) to unambiguously identify the structure of densely packed colloidal crystals assembled from latex spheres by confined convective assembly [78].

SRM has also contributed to an improved understanding of the relation between the (variation in) catalytic activity and morphology, structure and surface functionalization of nanoparticles.[81–83] Zhou et al. analysed the catalytic activity of single gold nanorods coated with a mesoporous silica, reaching a spatial resolution of ~40 nm and a temporal resolution of a single catalytic event.[84] Cang et al. detected single hot spots as small as 15 nm on silver nanoparticle clusters.[85] STED, PALM studies at sub-10 nm length scales[86] revealed a clear correlation between nanoparticle size and catalytic activity.[87–89] Temporal activity fluctuations of individual nanocatalysts have been related to surface restructuring,[86,90] and activity gradients to surface defects.

Care must be taken when interpreting SRM results of plasmonic nanoparticles, as the electrochemical and photophysical properties of the dyes are affected by the nature of the metallic surfaces[91,92] when the emission of the dye couples with the surface plasmon polaritons [93,94]. Probe's brightness and emission are modulated, with significant ramifications for the sensitivity of single molecule surface-enhanced Raman spectroscopy (SM-SERS) and the precision and accuracy of SRM imaging. A direct comparison between SM-SERS results of physisorbed and tethered Nile Blue revealed variations in the potential-dependent SERS intensity for chemisorbed but not for the physisorbed solvachromatic dye[91,92]. Direct evidence of mislocalization of dyes on plasmonic nanostructures was obtained from correlative AFM and SRM studies that revealed smaller-than-expected reconstructed images of gold nanorods[95]. To overcome such localization errors effectively, the emission of the fluorescent tags and the surface plasmons can be decoupled[93,94,96].

By contrast, at optimal dye–metal distances, the emissive coupling can be exploited to enhance fluorescence of the probe, to boost the photocatalyst activity and for site-specific functionalization. Highly system-specific sweet spots exist at which dye fluorescence enhancements are significant.[97] Profiting from this opportunity, Uji-i and co-workers imaged fluorescently tagged proteins on plasmonic nanowires[98]. Aramendía and co-workers used a similar two-laser activation strategy to convert spiropyran into its fluorescent merocyanine form on gold

nanorods[99]. The optimal dye–metal distance is short enough to promote fluorescence enhancement and long enough to limit fluorescence quenching. This offers maximal signal-to-noise ratios and improved localization precision.[100] Johlin et al. interrogated the near-field optical interactions between quantum emitters and nanostructures by directly measuring the modulation of probe brightness and its location relative to a silicon nanowire, aiming to image the strong, extended coupling between dipole-like sources and nanoscale antennas[101]. Simoncelli et al. developed a versatile plasmon-induced approach for the in situ surface-functionalization of gold nanoparticles. Such approach is based on a plasmon-selective photo-cleavage of surface thiols followed by ligand replacement with, for example, thiolated DNA oligonucleotides [102]. The success of the selective surface-functionalization was demonstrated by m-PAINT (metallic DNA-PAINT) upon binding to the surface strands of short, complementary strands carrying fluorophores that exhibit absorption and emission spectra decoupled and blue-shifted with respect to gold plasmonic modes (FIG. 2b) [12,67,103].

[H1] Imaging materials in action

In the previous section we describe the current state-of-the-art in the use of super resolution microscopy to study complex materials. However, these studies were often performed under conditions that are far from the real conditions of application (for example, in pure water). Notably, SRM is minimally invasive compared to other techniques, like electron microscopies and probe microscopies, and it can be often used to perform measurements of a material in its operational conditions. For example, SRM has been used to unveil the photophysical and electronic properties of devices made of conductive polymers[43] or perovskite[104]. SRM has had also a dramatic impact in the field of catalysis, in which single reactivity events have been probed with nanometric accuracy in catalytic reactors such as zeolites[84,105–109]. Finally, SRM mild imaging conditions allow one to study biomaterials in situ, for example in cellular environments. Being SRM initially developed for the imaging of biological structures, material–cell interactions have been the first targets to be studied.

In the next sections, we discuss the latest applications of SRM for the study of chemical biology and biomaterials. In particular, we repor on the study of cell uptake and trafficking; the study of stability and material alteration inside cells and probing material–biomolecules interactions (FIG. 3).

[H2] Cellular trafficking and localization

Understanding the exact localization of materials inside cells during cell internalization is crucial for applications such as drug and gene delivery, as different cell locations implies different biochemical environment. To this goal SMLM, SIM and STED have been employed, taking advantage of the peculiarities of the different techniques.

SIM is ideally suitable to perform live-cell studies due to the good temporal resolution and the minimum illumination power required. The exact intracellular localization of different nanomaterials has been determined

thanks to the high particle localization accuracy of SIM[110–113]. In addition to the exact localization of the nanomaterial, SIM enabled the motoring of its degradation over time, as fragments of 100-200 nm could be imaged. Another study reported on the internalization and trafficking of metal-organic frameworks in live cells avoiding any fixation aberration using SIM[111]. Nanoporous polyethylene glycol/poly-L-lysine particles complexed with siRNA targeting survivin have also been studied.[110] Trafficking of these particles inside the cells was investigated using a combination of deconvolution microscopy, fluorescence lifetime imaging microscopy (FLIM) and SIM. The latter provided insight on the final fate of the nanoparticles at long incubations times. Despite the limited special resolution compared to STED and SMLM, SIM is an optimal choice for long-term live cell study of intracellular trafficking due to the good temporal resolution and minimal phototoxicity.Reflected light SIM is an alternative approach that uses nanoparticles scattering to provide contrast. This technique was recently used to follow the internalization of iron and cerium oxide nanoparticles with 100 nm resolution[114].

STED was first used to study nanoparticle–cell interactions to demonstrate the nuclear localization and clustering of 30 nm fluorescent silica nanoparticles (SNPs) in Caco-2 cells[115,116]. More recently, Peuschel et al. used 3D STED to quantify the internalization of 25 nm and 85 nm SNPs in A549 cells[117] and differentiate between membrane-attached and internalized nanoparticles. A similar approach was also used to study the internalization and co-localization of carbon dots [118] and protein-based fluorescent nanoparticles[119]. In the latter case, nanoparticles were functionalised using [119] transferrin that was in turn labeled with a optimal STED dye (Atto647N).

The nanoparticle cellular uptake is well characterized with STED and not only internalization images could be attained, but also a colocalization study with endosome markers and inhibition and competition assays are included to prove Tf receptor-mediated cell entry.

STED spatial resolution enabled also the analysis of the nanoparticle clustering inside the endosomes. STED was also used to study the cellular internalization of albumin-stabilized fluorescent nanodiamonds.[120] The results revealed that albumin-decorated nanodiamonds do not cluster inside the cells, as opposed to bare nanodiamonds that agglomerate in the cytoplasm. Although in this study cells were fixed, the exceptional photostability of the nanodiamonds makes them ideal candidates for future long-term cell-tracking and/or in vivo applications. The enhanced resolution of STED compared to SIM allow us to visualize smaller particles as well as to distinguish single particles from their clusters, a key information that so far only by EM could provide. However, STED microscopy is limited by the choice of the labels and phototoxicity due to the required high illumination power hampers live-cell imaging .[121] To overcome this phototoxicity issue new illumination methods such as DyMin[122] and MINFIELD[123] that limit the sample exposure and improve phototoxicity have been proposed.

SMLM, in particular STORM, is so far the most employed method to study nanoparticles internalization and trafficking. STORM enabled the positioning and measurement of internalized particles down to 80nm, as in the

case of polystyrene particles of different sizes in HeLa cells.[124] Moreover 2-color STORM enabled the determination of colocalization assays with nanometer precision by assessing the interactions of the nanoparticles with specific subcellular organelles. This technique was performed both for the analysis of polystyene particles in HeLa cells, revealing the mechanism of endocytosis, and for polymer hydrogel particles in dendritic cells, where both the localization of nanoparticles and endocytic vesicles have been resolved.[125] By combining PALM and single particle tracking (SPT), Nienhaus and co-workers imaged clathrin-mediated endocytosis of fluorophore-labelled polystyrene nanoparticles.[126] PALM was used to visualize and investigate the formation of clathrin coated pits (CCPs, and SPT was used to record nanoparticle trajectories. This combined approach revealed that CCP is formed usually after the nanoparticle attached to the membrane, but occasionally the nanoparticle diffuses and uses a pre-formed CCP.

SMLM is the method endowed with the highest spatial resolution and therefore is ideal when high accuracy is needed. However, special care in the choice and conjugation of the label is needed to ensure optimal photoswitching. It should be noted that blinking can spontaneously occur for some types of photo-excited emitting particles like gold nanoparticles [127] or quantum dots [128], and could be used to image the aprticles' uptake [129]. Unfortunately, the slow imaging process of SMLM and the required high power hinder live-cell imaging and therefore all the current reports are limited to fixed cells.

Altogether SRM has led to remarkable improvement in the assessment of the intracellular localization and trafficking of nanoparticles compared to conventional fluorescence microscopy, being a valuable tool to dissect internalization pathways in cultured cells and, potentially, in vivo.[130,131]

[H2] Material stability

The enhanced resolution of SRM allows us to go beyond the bare visualization of nano-objects and their location, and probe several material properties in the cellular environment. This is particularly relevant for complex molecular architectures, designed to be responsive and adaptive in the biological environment. In this framework, controlling the stability of complex materials is crucial to obtain the desired biological effect. Unstable materials will result in premature disassembly and consequent inactivation. On the contrary, highly stable materials may lead to undesirable effects such as poor responsivity, poor payload release, bioaccumulation and toxicity. SRM can provide meaningful insights on the effect of the cellular environment on the stability of nanoparticles.

Methods based on SRM have been developed to quantitatively assess particle size and shape with nanometric resolution. Caruso and coworkers proposed a method based on SIM on fixed sample to perform a high-throughput quantification of particle size[132]. The group was able to quantify fluorescent particles of different compositions, structures (solid, porous, or hollow) and sizes (50–1000 nm) dispersed in either aqueous

solution or in cells. Despite its limited resolution, SIM is fast and easy to implement, and facilitates the quantification of nanoparticles in cells. In another report, researchers combined dSTORM with image analysis tools to assess the size of nanoparticles during internalization in different cell types[124]. Non-degradable and non-deformable nanoparticles have been used as a standard, comparing their nominal size measured in vitro using electron microscopy with the size measured inside cells using dSTORM. The results show an excellent agreement between the two measurements for nanoparticles ranging from 80 nm to 800 nm, demonstrating the potential of such technique for the assessment of the nanoparticle status inside cells. dSTORM has also been used to assess the stability of DiI-labeled quatsomes, a family of novel lipid nanoparticle[133]. Analysis of dSTORM images of quatsomes in vitro, before their incubation with cells, revealed the average size and number of labeled lipids. These data were compared with those obtained after incubation in HeLa cells and helped to distinguish intact functional quatsome from fragments of degraded particles. The destabilization of polymeric micelles upon incubation with serum was also studied using STORM that showed a lower degree of colocalization and smaller sizes structures compared to the freshly prepared micelles[134].

In addition to nanoparticle disassembly, other phenomena can occur during cell internalization. A relevant example is the particle deformation following internalization due to mechanical stress. Caruso and coworkers reported on the use of SIM to image the deformation of polymer capsules occurring inside cells [135]. Hollow spheres are more susceptible to mechanical stress and a high degree of compression was observed in different cell lines irrespective of the capsule shape, suggesting that the forces are cell-dependent. Moreover, the positioning of the cell obtained by SIM can be correlated with the capsule compression, revealing that the deformation starts from the plasma membrane, the first step of cell trafficking. In a revers approach, nanoparticles were used as sensor for cell mechanics[136]. By synthesizing capsules with controlled stiffness, the pressure exerted by cells can be calculated from the capsule deformation.

Although methods to assess fine assembly status of nanostructures inside cells need to be further optimized, the first applications of SRM to address stability and responsivity of complex materials in the biological environment are certainly encouraging.

[H2] Material–biomolecules interactions

Multicolor super resolution imaging facilitates the visualization of molecular interactions between a synthetic material and the biomolecules present in the biological fluids (such as blood) or in the cellular environment. Gaining information on these kind of interactions is crucial for the development of biomaterials for biomedical applications[137]. 2-color super-resolution measurements allow us to visualize the two partners of the interactions with nanometric resolution and potentially estimate the number of biomolecules involved.

STORM has been used to study in vitro nanoparticle–biomolecule interactions, such as those involved in the protein corona formation on different types of nanoparticles[138]. Thanks to the nanometric resolution of

STORM, the authors could study the corona formation of individual nanoparticles in contrast to previous ensemble techniques. This work unveiled for the first time heterogeneity in the number of proteins attached to the different nanoparticles of the same sample that could only be revealed thanks to the nanometric resolution of the technique. This information is of relevant interest when studying the functionality of the nanoparticles in vivo, as different protein corona may result in different performance of each individual nanoparticle [139]. STORM has also been used to study the penetration of different serum proteins within porous silica nanoparticles[140]. Penetration resulted to be dependent on the porous size and protein molecular weight, with most of the corona composed by low molecular weight proteins. STORM was used to observe the protein corona on TiO_2 nanoparticles. The study revealed that the proteins tend to form patches rather than homogenously cover the surface of the nanoparticles. SRM also helped to understand the protein corona turnover, which was complete after 24 hours, even for the hard corona, the layer formed by low abundance, higher affinity proteins.Protein corona on nanoparticles might have a positive effect as it can prevent plasma membrane lipid oxidation[141]. Lipid peroxidation resulted to be equally inhibited by an alumina-silica shell, by the presence of an antioxidant (Trolox) , as well as by the protein corona.

Nanoparticles are also exploited to study the cell response to different distribution of external ligands or substrate rigidity that are driven by the interaction between the nanomaterial and specific biomolecules, such as integrins. Cells can be grown on gels of controlled rigidity featuring equally-spaced functionalized nanoparticles on their surface that interact with cellular integrins. Interestingly, STORM revealed that integrin proteins organized into equally-spaced clusters (every 100 nm) reflected the underlying nanoparticles' pattern[142]. This work demonstrates that STORM is potentially compatible with imaging on gel substrates and can provide information on the organization of biomolecules interacting with nano-patterned materials on longer distances (100 nm scale). SRM is a powerful tool to understand material–cell interactions, which are highly important in the search of biomaterials for regenerative medicine, and to screen the effects of biomaterials on cell adhesome.

Finally, interactions between nanoparticles and cell membranes are crucial for selective drug delivery. The ability of nanoparticles to selectively bind cell membrane components and promote internalization is a key aspect of nanomedicine. To this goal, Chelladurai et al. studied the binding and diffusion of quantum dots in model membranes by combining STED with fluorescence correlation spectroscopy[143]. Interestingly, binding of quantum dots was enhanced in the two components phase-separated bilayers than in the one component fluid or gel-like bilayers. Also, the phase with the slower diffusivity became more fluid upon interaction with quantum dots in the multicomponent model membrane.

Understanding the complex network of molecular interactions of synthetic structures in the biological environment is a fundamental step towards the design of effective materials for a variety of applications and nanoscopy can play a pivotal role in this, thanks its unique multicolor ability and molecular resolution.

[H1] Conclusion and perspectives

The appealing properties of SRM, such as nanometer accuracy and multicolour ability, enabled the rapid spreading of this technique among several scientific communities. Despite the use of such methodologies for the study of synthetic complex materials is still in its infancy, the pioneering reports highlighted in this review demonstrate the potential of super-resolution imaging to unveil complex features of engineered materials. Nowadays super-resolution setups are widely available, making optical nanoscopy an important part of the arsenal of techniques available to chemists and materials scientists for complex materials characterization. In this framework, we envision that SRM will become in the next decade a key tool for the study of complex multicomponent materials. However, it is important to mention that nanoscopy still presents several limitations and therefore its use in material science should be carefully considered. For example, the low temporal resolution of SMLM makes it unsuitable for the imaging of highly dynamic systems. Moreover, most of the SRM techniques are not suitable for thick opaque samples and therefore not applicable to many bulk materials. Finally, SMLM and STED require special dyes and sample preparations, and longer sample optimization should be taken in account before to embark in such measurements. Especially sample preparations require the developments of specific protocols, as most of the protocols in the literature are currently optimized for biological specimens. At the same time, the need of new protocols opens exciting opportunities for chemists who can highly contribute to the development of new dyes for super-resolution imaging, labelling procedures, redox-controlled buffers to maximize the performances of SRM.

The choice of the super-resolution method is crucial and the ideal match between the scientific question and the type of sample on one side and the technique on the other has to be found. It has to be mentioned that the field of SRM is evolving rapidly and continuously improvements are introduced to overcome its limitations. Some of the latest development led to enhanced spatial resolution (down to 5 nm)[76], improved temporal resolution down to the millisecond range[144] and new methods able to image thick samples[145,146] .

The availability of new labels for both biological and synthetic systems is crucial for the improvement of the current SRM techniques. A remarkable advance towards the use of SRM for live cell imaging has been provided by self-blinking fluorophores[147] that enable dSTORM measurements without the use of any special buffer and under low power illumination. Furthermore, in the field of synthetic structures, a full integration between the labels and the materials, for example super-resolution autofluorescent materials, is desirable. To this aim, first reports using conjugated polymers[43–47], fluorescent nanodiamonds[148,149] or synthetic polymers that incorporate fluorescent units in the main backbones pave the way towards material-dye integration.

Despite these improvements, no technique alone will be able to cover all the spatial and temporal scales necessary to characterize complex materials. Therefore, advances in correlative microscopy represent a bright perspective. In correlative imaging, two different techniques are used to image — in a single setup or

separately — the same sample and the two images overlaid. By looking at the sample using different probes, different types of resolution and information are obtainable. Several techniques have been combined with SRM,[79] in particular electron microscopy[150–165] and atomic force microscopy[166–170]. However, the applications of correlative microscopy to synthetic samples are still limited[171–175] and tailored methods for the sample preparation, handling and imaging, are needed.

Altogether, a number of reports suggest a bright future for SRM for material chemistry in which microscopy will contribute to unveil the structure and properties of complex synthetic architectures and chemistry will provide new labels, labelling methods and sample treatments procedure to improve the performances of nanoscopy.

[H1] Competing interests

The authors declare no competing interests.

References:

1. Huang, B., Bates, M. & Zhuang, X. Super-Resolution Fluorescence Microscopy. *Annu. Rev. Biochem.* **78**, 993–1016 (2009).

2. Schermelleh, L., Heintzmann, R. & Leonhardt, H. A guide to super-resolution fluorescence microscopy. *J. Cell Biol.* **190**, 165–175 (2010).

3. Möckl, L., Lamb, D. C. & Bräuchle, C. Super-resolved Fluorescence Microscopy: Nobel Prize in Chemistry 2014 for Eric Betzig, Stefan Hell, and William E. Moerner. *Angew. Chem. Int. Ed.* **53**, 13972–13977 (2014).

4. Binnig, G., Quate, C. F. & Gerber, C. Atomic Force Microscope. *Phys. Rev. Lett.* **56**, 930–933 (1986).

5. Mathys, D. Die Entwicklung der Elektronenmikroskopie vom Bild über die Analyse zum Nanolabor. (2004).

6. Webber, M. J., Appel, E. A., Meijer, E. W. & Langer, R. Supramolecular biomaterials. *Nat. Mater.* **15**, 13–26 (2016).

7. Hyotyla, J. T. & Lim, R. Y. H. Atomic Force Microscopy (AFM). in *Supramolecular Chemistry* (John Wiley & Sons, Ltd, 2012).

8. Franken, L. E., Boekema, E. J. & Stuart, M. C. A. Transmission Electron Microscopy as a Tool for the Characterization of Soft Materials: Application and Interpretation. *Adv. Sci.* **4**, 1600476 (2017).

9. Lakowicz, J. R. *Principles of Fluorescence Spectroscopy*. (Springer, 2011).

10. Douglass, K. M., Sieben, C., Archetti, A., Lambert, A. & Manley, S. Super-resolution imaging of multiple cells by optimized flat-field epi-illumination. *Nat. Photonics* **10**, 705–708 (2016).

11. Bates, M., Dempsey, G. T., Chen, K. H. & Zhuang, X. Multicolor super-resolution fluorescence imaging via multi-parameter fluorophore detection. *Chemphyschem Eur. J. Chem. Phys. Phys. Chem.* **13**, 99–107 (2012).

12. Jungmann, R. *et al.* Multiplexed 3D cellular super-resolution imaging with DNA-PAINT and Exchange-PAINT. *Nat. Methods* **11**, 313–318 (2014).

13. Lee, S.-H., Shin, J. Y., Lee, A. & Bustamante, C. Counting single photoactivatable fluorescent molecules by photoactivated localization microscopy (PALM). *Proc. Natl. Acad. Sci.* **109**, 17436–17441 (2012).

14. Venkataramani, V., Herrmannsdörfer, F., Heilemann, M. & Kuner, T. SuReSim: simulating localization microscopy experiments from ground truth models. *Nat. Methods* **13**, 319–321 (2016).

15. Habuchi, S. Super-Resolution Molecular and Functional Imaging of Nanoscale Architectures in Life and Materials Science. *Front. Bioeng. Biotechnol.* **2**, (2014).

16. Van Loon, J., Kubarev, A. V. & Roeffaers, M. B. J. Correlating Catalyst Structure and Activity at the Nanoscale. *ChemNanoMat* **4**, 6–14 (2018).

17. Aida, T., Meijer, E. W. & Stupp, S. I. Functional Supramolecular Polymers. *Science* **335**, 813–817 (2012).

18. Albertazzi, L. *et al.* Probing exchange pathways in one-dimensional aggregates with super-resolution microscopy. *Science* **344**, 491–495 (2014).

19. Baker, M. B. *et al.* Consequences of chirality on the dynamics of a water-soluble supramolecular polymer. *Nat. Commun.* **6**, 6234 (2015).

20. Baker, M. B. *et al.* Exposing Differences in Monomer Exchange Rates of Multicomponent Supramolecular Polymers in Water. *ChemBioChem* **17**, 207–213 (2016).

21. Aloi, A. *et al.* Imaging Nanostructures by Single-molecule Localization Microscopy in Organic Solvents. *J. Am. Chem. Soc.* **138**, 2953-2956 (2016).

22. Boott, C. E. *et al.* In Situ Visualization of Block Copolymer Self-Assembly in Organic Media by Super-Resolution Fluorescence Microscopy. *Chem. Weinh. Bergstr. Ger.* **21**, 18539–18542 (2015).

23. Adelizzi, B. *et al.* Painting Supramolecular Polymers in Organic Solvents by Super-resolution Microscopy. *ACS Nano* **12**, 4431–4439 (2018).

24. Hendrikse, S. I. S. *et al.* Controlling and tuning the dynamic nature of supramolecular polymers in aqueous solutions. *Chem. Commun.* **53**, 2279–2282 (2017).

25. Lee, O.-S., Stupp, S. I. & Schatz, G. C. Atomistic Molecular Dynamics Simulations of Peptide Amphiphile Self-Assembly into Cylindrical Nanofibers. *J. Am. Chem. Soc.* **133**, 3677–3683 (2011).

26. Aloi, A., Vilanova, N., Albertazzi, L. & Voets, I. K. iPAINT: a general approach tailored to image the topology of interfaces with nanometer resolution. *Nanoscale* **8**, 8712–8716 (2016).

27. Merdasa, A. *et al.* Single Lévy States–Disorder Induced Energy Funnels in Molecular Aggregates. *Nano Lett.* **14**, 6774–6781 (2014).

28. Onogi, S. *et al.* In situ real-time imaging of self-sorted supramolecular nanofibres. *Nat. Chem.* **8**, 743–752 (2016).

29. Tønnesen, J., Inavalli, V. V. G. K. & Nägerl, U. V. Super-Resolution Imaging of the Extracellular Space in Living Brain Tissue. *Cell* **172**, 1108-1121.e15 (2018).

30. Schacher Felix H., Rupar Paul A. & Manners Ian. Functional Block Copolymers: Nanostructured Materials with Emerging Applications. *Angew. Chem. Int. Ed.* **51**, 7898–7921 (2012).

31. Qiu, H. *et al.* Uniform patchy and hollow rectangular platelet micelles from crystallizable polymer blends. *Science* **352**, 697–701 (2016).

32. Ullal, C. K., Schmidt, R., Hell, S. W. & Egner, A. Block Copolymer Nanostructures Mapped by Far-Field Optics. *Nano Lett.* **9**, 2497–2500 (2009).

33. Yan, J. *et al.* Optical Nanoimaging for Block Copolymer Self-Assembly. *J. Am. Chem. Soc.* **137**, 2436–2439 (2015).

34. González-Aramundiz, J. V., Lozano, M. V., Sousa-Herves, A., Fernandez-Megia, E. & Csaba, N. Polypeptides and polyaminoacids in drug delivery. *Expert Opin. Drug Deliv.* **9**, 183–201 (2012).

35. Beun, L. H., Albertazzi, L., van der Zwaag, D., de Vries, R. & Cohen Stuart, M. A. Unidirectional Living Growth of Self-Assembled Protein Nanofibrils Revealed by Super-resolution Microscopy. *ACS Nano* **10**, 4973–4980 (2016).

36. Duro-Castano Aroa *et al.* Capturing "Extraordinary" Soft-Assembled Charge-Like Polypeptides as a Strategy for Nanocarrier Design. *Adv. Mater.* **29**, 1702888 (2017).

37. Muls Benoît *et al.* Direct Measurement of the End-to-End Distance of Individual Polyfluorene Polymer Chains. *ChemPhysChem* **6**, 2286–2294 (2005).

38. Vacha, M. & Habuchi, S. Conformation and physics of polymer chains: a single-molecule perspective. *NPG Asia Mater.* **2**, 134–142 (2010).

39. Aoki, H., Mori, K. & Ito, S. Conformational analysis of single polymer chains in three dimensions by super-resolution fluorescence microscopy. *Soft Matter* **8**, 4390–4395 (2012).

40. Gramlich, M. W., Bae, J., Hayward, R. C. & Ross, J. L. Fluorescence imaging of nanoscale domains in polymer blends using stochastic optical reconstruction microscopy (STORM). *Opt. Express* **22**, 8438–8450 (2014).

41. ONeil, C. E., Jackson, J. M., Shim, S.-H. & Soper, S. A. Interrogating Surface Functional Group Heterogeneity of Activated Thermoplastics Using Super-Resolution Fluorescence Microscopy. *Anal. Chem.* **88**, 3686–3696 (2016).

42. Bolinger, J. C., Traub, M. C., Adachi, T. & Barbara, P. F. Ultralong-Range Polaron-Induced Quenching of Excitons in Isolated Conjugated Polymers. *Science* **331**, 565–567 (2011).

43. Habuchi, S., Onda, S. & Vacha, M. Mapping the emitting sites within a single conjugated polymer molecule. *Chem. Commun.* **0**, 4868–4870 (2009).

44. Habuchi, S., Onda, S. & Vacha, M. Molecular weight dependence of emission intensity and emitting sites distribution within single conjugated polymer molecules. *Phys. Chem. Chem. Phys.* **13**, 1743–1753 (2011).

45. Park, H., Hoang, D. T., Paeng, K. & Kaufman, L. J. Localizing Exciton Recombination Sites in Conformationally Distinct Single Conjugated Polymers by Super-resolution Fluorescence Imaging. *ACS Nano* **9**, 3151–3158 (2015).

46. Penwell, S. B., Ginsberg, L. D. S. & Ginsberg, N. S. Bringing Far-Field Subdiffraction Optical Imaging to Electronically Coupled Optoelectronic Molecular Materials Using Their Endogenous Chromophores. *J. Phys. Chem. Lett.* **6**, 2767–2772 (2015).

47. King, J. T. & Granick, S. Operating organic light-emitting diodes imaged by super-resolution spectroscopy. *Nat. Commun.* **7**, 11691 (2016).

48. Tian, Z., Li, A. D. Q. & Hu, D. Super-resolution fluorescence nanoscopy applied to imaging core–shell photoswitching nanoparticles and their self-assemblies. *Chem. Commun.* **47**, 1258–1260 (2011).

49. Hu, D., Tian, Z., Wu, W., Wan, W. & Li, A. D. Q. Photoswitchable Nanoparticles Enable High-Resolution Cell Imaging: PULSAR Microscopy. *J. Am. Chem. Soc.* **130**, 15279–15281 (2008).

50. Gong, W.-L. *et al.* Single-wavelength-controlled in situ dynamic super-resolution fluorescence imaging for block copolymer nanostructures via blue-light-switchable FRAP. *Photochem. Photobiol. Sci. Off. J. Eur. Photochem. Assoc. Eur. Soc. Photobiol.* **15**, 1433-1441 (2016).

50. Nevskyi, O., Sysoiev, D., Oppermann, A., Huhn, T. & Wöll D. Nanoscopic Visualization of Soft Matter Using Fluorescent Diarylethene Photoswitches. *Angew. Chem. Int. Ed.* **55**, 12698–12702 (2016).

52. Hu, D., Tian, Z., Wu, W., Wan, W. & Li, A. D. Q. Photoswitchable Nanoparticles Enable High-Resolution Cell Imaging: The PULSAR Microscopy. *J. Am. Chem. Soc.* **130**, 15279–15281 (2008).

53. Urban, B. E. *et al.* Subsurface Super-resolution Imaging of Unstained Polymer Nanostructures. *Sci. Rep.* **6**, 28156 (2016).

54. Barenholz, Y. Doxil®--the first FDA-approved nano-drug: lessons learned. *J. Control. Release Off. J. Control. Release Soc.* **160**, 117–134 (2012).

55. Sharonov, A. & Hochstrasser, R. M. Wide-field subdiffraction imaging by accumulated binding of diffusing probes. *Proc. Natl. Acad. Sci. U. S. A.* **103**, 18911–18916 (2006).

56. Kuo, C. & Hochstrasser, R. M. Super-resolution Microscopy of Lipid Bilayer Phases. *J. Am. Chem. Soc.* **133**, 4664–4667 (2011).

57. Bongiovanni, M. N. *et al.* Multi-dimensional super-resolution imaging enables surface hydrophobicity mapping. *Nat. Commun.* **7**, 13544 (2016).

58. Yan, R., Moon, S., Kenny, S. J. & Xu, K. Spectrally Resolved and Functional Super-resolution Microscopy via Ultrahigh-Throughput Single-Molecule Spectroscopy. *Acc. Chem. Res.* **51**, 697–705 (2018).

59. Boreham, A., Volz, P., Peters, D., Keck, C. M. & Alexiev, U. Determination of nanostructures and drug distribution in lipid nanoparticles by single molecule microscopy. *Eur. J. Pharm. Biopharm.* **110**, 31–38 (2017).

60. Belfiore, L., Spenkelink, L. M., Ranson, M., van Oijen, A. M. & Vine, K. L. Quantification of ligand density and stoichiometry on the surface of liposomes using single-molecule fluorescence imaging. *J. Controlled Release* **278**, 80–86 (2018).

61. Rothemund, P. W. K. Folding DNA to create nanoscale shapes and patterns. *Nature* **440**, 297–302 (2006).

62. Saccà, B. & Niemeyer, C. M. DNA origami: the art of folding DNA. *Angew. Chem. Int. Ed Engl.* **51**, 58–66 (2012).

63. Graugnard, E., Hughes, W. L., Jungmann, R., Kostiainen, M. A. & Linko, V. Nanometrology and super-resolution imaging with DNA. *MRS Bull.* **42**, 951–959 (2017).

64. Steinhauer, C., Jungmann, R., Sobey, T., Simmel, F. & Tinnefeld, P. DNA Origami as a Nanoscopic Ruler for Super-Resolution Microscopy. *Angew. Chem. Int. Ed.* **48**, 8870–8873 (2009).

65. Schmied, J. J. *et al.* DNA origami nanopillars as standards for three-dimensional superresolution microscopy. *Nano Lett.* **13**, 781–785 (2013).

66. Schmied, J. J. *et al.* Fluorescence and super-resolution standards based on DNA origami. *Nat. Methods* **9**, 1133–1134 (2012).

67. Jungmann, R. *et al.* Single-Molecule Kinetics and Super-Resolution Microscopy by Fluorescence Imaging of Transient Binding on DNA Origami. *Nano Lett.* **10**, 4756–4761 (2010).

68. Smith, D. M. *et al.* A structurally variable hinged tetrahedron framework from DNA origami. *J. Nucleic Acids* **2011**, 360954 (2011).

69. Scheible, M. B. *et al.* A Compact DNA Cube with Side Length 10 nm. *Small Weinh. Bergstr. Ger.* **11**, 5200–5205 (2015).

70. Chen, J., Bremauntz, A., Kisley, L., Shuang, B. & Landes, C. F. Super-Resolution mbPAINT for Optical Localization of Single-Stranded DNA. *ACS Appl. Mater. Interfaces* **5**, 9338–9343 (2013).

71. Knudsen, J. B. *et al.* Routing of individual polymers in designed patterns. *Nat. Nanotechnol.* **10**, 892–898 (2015).

72. Schueder, F. *et al.* Multiplexed 3D super-resolution imaging of whole cells using spinning disk confocal microscopy and DNA-PAINT. *Nat. Commun.* **8**, (2017).

73. Auer, A., Strauss, M. T., Schlichthaerle, T. & Jungmann, R. Fast, Background-Free DNA-PAINT Imaging Using FRET-Based Probes. *Nano Lett.* **17**, 6428–6434 (2017).

74. Karathanasis, C., Fricke, F., Hummer, G. & Heilemann, M. Molecule Counts in Localization Microscopy with Organic Fluorophores. *ChemPhysChem* **18**, 942–948 (2017).

75. Beater, S., Holzmeister, P., Pibiri, E., Lalkens, B. & Tinnefeld, P. Choosing dyes for cw-STED nanoscopy using self-assembled nanorulers. *Phys. Chem. Chem. Phys. PCCP* **16**, 6990–6996 (2014).

76. Dai, M., Jungmann, R. & Yin, P. Optical imaging of individual biomolecules in densely packed clusters. *Nat. Nanotechnol.* **11**, 798–807 (2016).

77. Delcanale, P., Miret-Ontiveros, B., Arista-Romero, M., Pujals, S. & Albertazzi, L. Nanoscale Mapping Functional Sites on Nanoparticles by Points Accumulation for Imaging in Nanoscale Topography (PAINT). *ACS Nano* **12**, 7629–7637 (2018).

78. Harke, B., Ullal, C. K., Keller, J. & Hell, S. W. Three-Dimensional Nanoscopy of Colloidal Crystals. *Nano Lett.* **8**, 1309–1313 (2008).

79. Hauser, M. *et al.* Correlative Super-Resolution Microscopy: New Dimensions and New Opportunities. *Chem. Rev.* **117**, 7428-7456 (2017).

80. Bon, P. *et al.* Three-dimensional nanometre localization of nanoparticles to enhance super-resolution microscopy. *Nat. Commun.* **6**, 7764 (2015).

81. Xu, W., Kong, J. S., Yeh, Y.-T. E. & Chen, P. Single-molecule nanocatalysis reveals heterogeneous reaction pathways and catalytic dynamics. *Nat. Mater.* **7**, 992–996 (2008).

82. Chen, T., Zhang, Y. & Xu, W. Single-Molecule Nanocatalysis Reveals Catalytic Activation Energy of Single Nanocatalysts. *J. Am. Chem. Soc.* **138**, 12414–12421 (2016).

83. Zhou, X., Choudhary, E., Andoy, N. M., Zou, N. & Chen, P. Scalable Parallel Screening of Catalyst Activity at the Single-Particle Level and Subdiffraction Resolution. *ACS Catal.* **3**, 1448–1453 (2013).

84. Zhou, X. *et al.* Quantitative super-resolution imaging uncovers reactivity patterns on single nanocatalysts. *Nat. Nanotechnol.* **7**, 237–241 (2012).

85. Cang, H. *et al.* Probing the electromagnetic field of a 15-nanometre hotspot by single molecule imaging. *Nature* **469**, 385–388 (2011).

86. Xu, W., Kong, J. S. & Chen, P. Probing the catalytic activity and heterogeneity of Au-nanoparticles at the single-molecule level. *Phys. Chem. Chem. Phys.* **11**, 2767–2778 (2009).

87. Zhou, X., Xu, W., Liu, G., Panda, D. & Chen, P. Size-Dependent Catalytic Activity and Dynamics of Gold Nanoparticles at the Single-Molecule Level. *J. Am. Chem. Soc.* **132**, 138–146 (2010).

88. Chen, T., Zhang, Y. & Xu, W. Size-dependent catalytic kinetics and dynamics of Pd nanocubes: a single-particle study. *Phys. Chem. Chem. Phys.* **18**, 22494–22502 (2016).

89. Shen, H., Zhou, X., Zou, N. & Chen, P. Single-Molecule Kinetics Reveals a Hidden Surface Reaction Intermediate in Single-Nanoparticle Catalysis. *J. Phys. Chem. C* **118**, 26902–26911 (2014).

90. Han, K. S., Liu, G., Zhou, X., Medina, R. E. & Chen, P. How Does a Single Pt Nanocatalyst Behave in Two Different Reactions? A Single-Molecule Study. *Nano Lett.* **12**, 1253–1259 (2012).

91. Wilson, A. J., Molina, N. Y. & Willets, K. A. Modification of the Electrochemical Properties of Nile Blue through Covalent Attachment to Gold As Revealed by Electrochemistry and SERS. *J. Phys. Chem. C* **120**, 21091–21098 (2016).

92. Wilson, A. J. & Willets, K. A. Unforeseen distance-dependent SERS spectroelectrochemistry from surface-tethered Nile Blue: the role of molecular orientation. *Analyst* **141**, 5144–5151 (2016).

93. Titus, E. J., Weber, M. L., Stranahan, S. M. & Willets, K. A. Super-Resolution SERS Imaging beyond the Single-Molecule Limit: An Isotope-Edited Approach. *Nano Lett.* **12**, 5103–5110 (2012).

94. Willets, K. A., Wilson, A. J., Sundaresan, V. & Joshi, P. B. Super-Resolution Imaging and Plasmonics. *Chem. Rev.* **117**, 7538–7582 (2017).

95. Blythe, K. L., Mayer, K. M., Weber, M. L. & Willets, K. A. Ground state depletion microscopy for imaging interactions between gold nanowires and fluorophore-labeled ligands. *Phys. Chem. Chem. Phys.* **15**, 4136–4145 (2013).

96. Lim, K. *et al.* Nanostructure-Induced Distortion in Single-Emitter Microscopy. *Nano Lett.* **16**, 5415–5419 (2016).

97. Thompson, R. E., Larson, D. R. & Webb, W. W. Precise nanometer localization analysis for individual fluorescent probes. *Biophys. J.* **82**, 2775–2783 (2002).

98. Lin, H. *et al.* Mapping of Surface-Enhanced Fluorescence on Metal Nanoparticles using Super-Resolution Photoactivation Localization Microscopy. *ChemPhysChem* **13**, 973–981 (2012).

99. Simoncelli, S., Roberti, M. J., Araoz, B., Bossi, M. L. & Aramendía, P. F. Mapping the Fluorescence Performance of a Photochromic–Fluorescent System Coupled with Gold Nanoparticles at the Single-Molecule–Single-Particle Level. *J. Am. Chem. Soc.* **136**, 6878–6880 (2014).

100. Fu, B., Flynn, J. D., Isaacoff, B. P., Rowland, D. J. & Biteen, J. S. Super-Resolving the Distance-Dependent Plasmon-Enhanced Fluorescence of Single Dye and Fluorescent Protein Molecules. *J. Phys. Chem. C* **119**, 19350–19358 (2015).

101. Johlin, E. *et al.* Super-resolution imaging of light–matter interactions near single semiconductor nanowires. *Nat. Commun.* **7**, 13950 (2016).

102. Simoncelli, S., Li, Y., Cortés, E. & Maier, S. A. Nanoscale Control of Molecular Self-Assembly Induced by Plasmonic Hot-Electron Dynamics. *ACS Nano* **12**, 2184–2192 (2018).

103. Taylor, A., Verhoef, R., Beuwer, M., Wang, Y. & Zijlstra, P. All-Optical Imaging of Gold Nanoparticle Geometry Using Super-Resolution Microscopy. *J. Phys. Chem. C Nanomater. Interfaces* **122**, 2336–2342 (2018).

104. Yuan, H. *et al.* Imaging Heterogeneously Distributed Photo-Active Traps in Perovskite Single Crystals. *Adv. Mater.* **30**, 1705494 (2018)

105. Ristanović, Z. *et al.* High-Resolution Single-Molecule Fluorescence Imaging of Zeolite Aggregates within Real-Life Fluid Catalytic Cracking Particles. *Angew. Chem. Int. Ed.* **54**, 1836–1840 (2015).

106. Ristanović, Z. *et al.* Quantitative 3D Fluorescence Imaging of Single Catalytic Turnovers Reveals Spatiotemporal Gradients in Reactivity of Zeolite H-ZSM-5 Crystals upon Steaming. *J. Am. Chem. Soc.* **137**, 6559–6568 (2015).

107. Roeffaers, M. B. J. *et al.* Super-Resolution Reactivity Mapping of Nanostructured Catalyst Particles. *Angew. Chem. Int. Ed.* **48**, 9285–9289 (2009).

108. Hendriks, F. C. *et al.* Integrated Transmission Electron and Single-Molecule Fluorescence Microscopy Correlates Reactivity with Ultrastructure in a Single Catalyst Particle. *Angew. Chem. Int. Ed.* **57**, 257–261 (2018).

109. Roeffaers, M. B. J. *et al.* Spatially resolved observation of crystal-face-dependent catalysis by single turnover counting. *Nature* **439**, 572–575 (2006).

110. Cavalieri, F. *et al.* Redox-Sensitive PEG–Polypeptide Nanoporous Particles for Survivin Silencing in Prostate Cancer Cells. *Biomacromolecules* **16**, 2168–2178 (2015).

111. Teplensky, M. H. *et al.* Temperature Treatment of Highly Porous Zirconium-Containing Metal–Organic Frameworks Extends Drug Delivery Release. *J. Am. Chem. Soc.* **139**, 7522–7532 (2017).

112. Tolstik, E. *et al.* Studies of silicon nanoparticles uptake and biodegradation in cancer cells by Raman spectroscopy. *Nanomedicine Nanotechnol. Biol. Med.* **12**, 1931–1940 (2016).

113. Tolstik, E. *et al.* Linear and Non-Linear Optical Imaging of Cancer Cells with Silicon Nanoparticles. *Int. J. Mol. Sci.* **17**, (2016).

114. Guggenheim, E. J. *et al.* Comparison of Confocal and Super-Resolution Reflectance Imaging of Metal Oxide Nanoparticles. *PLOS ONE* **11**, e0159980 (2016).

115. Schübbe, S. *et al.* Size-Dependent Localization and Quantitative Evaluation of the Intracellular Migration of Silica Nanoparticles in Caco-2 Cells. *Chem. Mater.* **24**, 914–923 (2012).

116. Schübbe, S., Cavelius, C., Schumann, C., Koch, M. & Kraegeloh, A. STED Microscopy to Monitor Agglomeration of Silica Particles Inside A549 Cells. *Adv. Eng. Mater.* **12**, 417–422 (2010).

117. Peuschel, H., Ruckelshausen, T., Cavelius, C. & Kraegeloh, A. Quantification of Internalized Silica Nanoparticles via STED Microscopy. *BioMed Res. Int.* **2015**, (2015).

118. Leménager, G., Luca, E. D., Sun, Y.-P. & Pompa, P. P. Super-resolution fluorescence imaging of biocompatible carbon dots. *Nanoscale* **6**, 8617–8623 (2014).

119. Shang, L. *et al.* Protein-based fluorescent nanoparticles for super-resolution STED imaging of live cells. *Chem. Sci.* **8**, 2396–2400 (2017).

120. Tzeng, Y.-K. *et al.* Superresolution imaging of albumin-conjugated fluorescent nanodiamonds in cells by stimulated emission depletion. *Angew. Chem. Int. Ed Engl.* **50**, 2262–2265 (2011).

121. Wäldchen, S., Lehmann, J., Klein, T., Linde, S. van de & Sauer, M. Light-induced cell damage in live-cell super-resolution microscopy. *Sci. Rep.* **5**, 15348 (2015).

122. Heine, J. *et al.* Adaptive-illumination STED nanoscopy. *Proc. Natl. Acad. Sci.* **114**, 9797-9802 (2017)

123. Göttfert, F. *et al.* Strong signal increase in STED fluorescence microscopy by imaging regions of subdiffraction extent. *Proc. Natl. Acad. Sci.* **114**, 2125–2130 (2017).

124. van der Zwaag, D. *et al.* Super Resolution Imaging of Nanoparticles Cellular Uptake and Trafficking. *ACS Appl. Mater. Interfaces* **8**, 6391–6399 (2016).

125. De Koker, S. *et al.* Engineering Polymer Hydrogel Nanoparticles for Lymph Node-Targeted Delivery. *Angew. Chem. Int. Ed Engl.* **55**, 1334–1339 (2016).

126. Li, Y., Shang, L. & Nienhaus, G. U. Super-resolution imaging-based single particle tracking reveals dynamics of nanoparticle internalization by live cells. *Nanoscale* **8**, 7423–7429 (2016).

127. Geddes, C. D., Parfenov, A., Gryczynski, I. & Lakowicz, J. R. Luminescent blinking of gold nanoparticles. *Chem. Phys. Lett.* **380**, 269–272 (2003).

128. Kuno, M., Fromm, D. P., Hamann, H. F., Gallagher, A. & Nesbitt, D. J. "On"/"off" fluorescence intermittency of single semiconductor quantum dots. *J. Chem. Phys.* **115**, 1028–1040 (2001).

129. Moser, F. *et al.* Cellular Uptake of Gold Nanoparticles and Their Behavior as Labels for Localization Microscopy. *Biophys. J.* **110**, 947–953 (2016).

130. Wegner, W. *et al.* In vivo mouse and live cell STED microscopy of neuronal actin plasticity using far-red emitting fluorescent proteins. *Sci. Rep.* **7**, 11781 (2017).

131. Wegner, W., Mott, A. C., Grant, S. G. N., Steffens, H. & Willig, K. I. In vivo STED microscopy visualizes PSD95 sub-structures and morphological changes over several hours in the mouse visual cortex. *Sci. Rep.* **8**, 219 (2018).

132. Cui, J. *et al.* Immobilized Particle Imaging for Quantification of Nano- and Microparticles. *Langmuir* **32**, 3532–3540 (2016).

133. Ardizzone Antonio *et al.* Nanostructuring Lipophilic Dyes in Water Using Stable Vesicles, Quatsomes, as Scaffolds and Their Use as Probes for Bioimaging. *Small* **0**, 1703851 (2018).

134. Krivitsky, A. *et al.* Amphiphilic poly(α)glutamate polymeric micelles for systemic administration of siRNA to tumors. *Nanomedicine Nanotechnol. Biol. Med.* **14**, 303–315 (2018).

135. Chen, X. *et al.* Analysing intracellular deformation of polymer capsules using structured illumination microscopy. *Nanoscale* **8**, 11924–11931 (2016).

136. Chen, X. *et al.* Probing cell internalisation mechanics with polymer capsules. *Nanoscale* **8**, 17096–17101 (2016).

137. Wilhelm, S. *et al.* Analysis of nanoparticle delivery to tumours. *Nat. Rev. Mater.* **1**, 16014 (2016).

138. Ke, P. C., Lin, S., Parak, W. J., Davis, T. P. & Caruso, F. A Decade of the Protein Corona. *ACS Nano* **11**, 11773–11776 (2017).

139. Feiner-Gracia, N. *et al.* Super-Resolution Microscopy Unveils Dynamic Heterogeneities in Nanoparticle Protein Corona. *Small* **13**, (2017).

140. Clemments, A. M., Botella, P. & Landry, C. C. Spatial Mapping of Protein Adsorption on Mesoporous Silica Nanoparticles by Stochastic Optical Reconstruction Microscopy. *J. Am. Chem. Soc.* **139**, 3978–3981 (2017).

141. Runa, S., Lakadamyali, M., Kemp, M. L. & Payne, C. K. TiO2 Nanoparticle-Induced Oxidation of the Plasma Membrane: Importance of the Protein Corona. *J. Phys. Chem. B* **121**, 8619–8625 (2017).

142. Oria, R. *et al.* Force loading explains spatial sensing of ligands by cells. *Nature* **552**, 219–224 (2017).

143. Chelladurai, R., Debnath, K., Jana, N. R. & Basu, J. K. Nanoscale Heterogeneities Drive Enhanced Binding and Anomalous Diffusion of Nanoparticles in Model Biomembranes. *Langmuir* **34**, 1691–1699 (2018).

144. Chmyrov, A. *et al.* Nanoscopy with more than 100,000 'doughnuts'. *Nat. Methods* **10**, 737–740 (2013).

145. Winter, P. W. *et al.* Incoherent structured illumination improves optical sectioning and contrast in multiphoton super-resolution microscopy. *Opt. Express* **23**, 5327–5334 (2015).

146. Izeddin, I. *et al.* PSF shaping using adaptive optics for three-dimensional single-molecule super-resolution imaging and tracking. *Opt. Express* **20**, 4957–4967 (2012).

147. Uno, S. *et al.* A spontaneously blinking fluorophore based on intramolecular spirocyclization for live-cell super-resolution imaging. *Nat. Chem.* **6**, 681–689 (2014).

148. Hsiao, W. W.-W., Hui, Y. Y., Tsai, P.-C. & Chang, H.-C. Fluorescent Nanodiamond: A Versatile Tool for Long-Term Cell Tracking, Super-Resolution Imaging, and Nanoscale Temperature Sensing. *Acc. Chem. Res.* **49**, 400–407 (2016).

149. Kianinia, M. *et al.* All-optical control and super-resolution imaging of quantum emitters in layered materials. *Nat. Commun.* **9**, 874 (2018).

150. Betzig, E. *et al.* Imaging Intracellular Fluorescent Proteins at Nanometer Resolution. *Science* **313**, 1642–1645 (2006).

151. Watanabe, S. *et al.* Protein localization in electron micrographs using fluorescence nanoscopy. *Nat. Methods* **8**, 80–84 (2011).

152. Kopek, B. G., Shtengel, G., Xu, C. S., Clayton, D. A. & Hess, H. F. Correlative 3D superresolution fluorescence and electron microscopy reveal the relationship of mitochondrial nucleoids to membranes. *Proc. Natl. Acad. Sci.* **109**, 6136–6141 (2012).

153. Kopek, B. G., Shtengel, G., Grimm, J. B., Clayton, D. A. & Hess, H. F. Correlative Photoactivated Localization and Scanning Electron Microscopy. *PLOS ONE* **8**, e77209 (2013).

154. Suleiman, H. *et al.* Nanoscale protein architecture of the kidney glomerular basement membrane. *eLife* **2**, e01149 (2013).

155. Sochacki, K. A., Shtengel, G., Engelenburg, S. B. van, Hess, H. F. & Taraska, J. W. Correlative super-resolution fluorescence and metal-replica transmission electron microscopy. *Nat. Methods* **11**, 305–308 (2014).

156. Engelenburg, S. B. V. *et al.* Distribution of ESCRT Machinery at HIV Assembly Sites Reveals Virus Scaffolding of ESCRT Subunits. *Science* **343**: 653-656 (2014).

157. Perkovic, M. *et al.* Correlative Light- and Electron Microscopy with chemical tags. *J. Struct. Biol.* **186**, 205–213 (2014).

158. Chang, Y.-W. *et al.* Correlated cryogenic photoactivated localization microscopy and cryo-electron tomography. *Nat. Methods* **11**, 737–739 (2014).

159. Löschberger, A., Franke, C., Krohne, G., Linde, S. van de & Sauer, M. Correlative super-resolution fluorescence and electron microscopy of the nuclear pore complex with molecular resolution. *J Cell Sci* **127**, 4351–4355 (2014).

160. Jord, A. A. *et al.* Centriole amplification by mother and daughter centrioles differs in multiciliated cells. *Nature* **516**, 104–107 (2014).

161. Paez-Segala, M. G. *et al.* Fixation-resistant photoactivatable fluorescent proteins for CLEM. *Nat. Methods* **12**, 215–218 (2015).

162. Johnson, E. *et al.* Correlative in-resin super-resolution and electron microscopy using standard fluorescent proteins. *Sci. Rep.* **5**, 9583 (2015).

163. Kim, D. *et al.* Correlative Stochastic Optical Reconstruction Microscopy and Electron Microscopy. *PLOS ONE* **10**, e0124581 (2015).

164. Wojcik, M., Hauser, M., Li, W., Moon, S. & Xu, K. Graphene-enabled electron microscopy and correlated super-resolution microscopy of wet cells. *Nat. Commun.* **6**, 7384 (2015).

165. Liu, B. *et al.* Three-dimensional super-resolution protein localization correlated with vitrified cellular context. *Sci. Rep.* **5**, 13017 (2015).

166. Harke, B., Chacko, J. V., Haschke, H., Canale, C. & Diaspro, A. A novel nanoscopic tool by combining AFM with STED microscopy. *Opt. Nanoscopy* **1**, 3 (2012).

167. Odermatt, P. D. *et al.* High-Resolution Correlative Microscopy: Bridging the Gap between Single Molecule Localization Microscopy and Atomic Force Microscopy. *Nano Lett.* **15**, 4896–4904 (2015).

168. Chacko, J. V., Canale, C., Harke, B. & Diaspro, A. Sub-Diffraction Nano Manipulation Using STED AFM. *PLOS ONE* **8**, e66608 (2013).

169. Monserrate Aitor, Casado Santiago & Flors Cristina. Correlative Atomic Force Microscopy and Localization-Based Super-Resolution Microscopy: Revealing Labelling and Image Reconstruction Artefacts. *ChemPhysChem* **15**, 647–650 (2013).

170. Chacko, J. V., Zanacchi, F. C. & Diaspro, A. Probing Cytoskeletal Structures by Coupling Optical Superresolution and AFM Techniques for a Correlative Approach. *Cytoskelet. Hoboken Nj* **70**, 729–740 (2013).

171. Frasconi, M. *et al.* Multi-Functionalized Carbon Nano-onions as Imaging Probes for Cancer Cells. *Chem. Weinh. Bergstr. Ger.* **21**, 19071–19080 (2015).

172. Fenaroli, F. *et al.* Nanoparticles as Drug Delivery System against Tuberculosis in Zebrafish Embryos: Direct Visualization and Treatment. *ACS Nano* **8**, 7014–7026 (2014).

173. Othman, B. A. *et al.* Correlative Light-Electron Microscopy Shows RGD-Targeted ZnO Nanoparticles Dissolve in the Intracellular Environment of Triple Negative Breast Cancer Cells and Cause Apoptosis with Intratumor Heterogeneity. *Adv. Healthc. Mater.* **5**, 1310–1325 (2016).

174. Reifarth, M. *et al.* Cellular uptake of PLA nanoparticles studied by light and electron microscopy: synthesis, characterization and biocompatibility studies using an iridium(III) complex as correlative label. *Chem. Commun.* **52**, 4361–4364 (2016).

175. Kempen, P. J. *et al.* A correlative optical microscopy and scanning electron microscopy approach to locating nanoparticles in brain tumors. *Micron* **68**, 70–76 (2015).

176. Gustafsson, M. G. L. Surpassing the lateral resolution limit by a factor of two using structured illumination microscopy. *J. Microsc.* **198**, 82–87 (2000).

177. Godin, A. G., Lounis, B. & Cognet, L. Super-resolution Microscopy Approaches for Live Cell Imaging. *Biophys. J.* **107**, 1777–1784 (2014).

178. Gustafsson, M. G. L. Nonlinear structured-illumination microscopy: Wide-field fluorescence imaging with theoretically unlimited resolution. *Proc. Natl. Acad. Sci.* **102**, 13081–13086 (2005).

179. York, A. G. *et al.* Instant super-resolution imaging in live cells and embryos via analog image processing. *Nat. Methods* **10**, 1122–1126 (2013).

180. Hell, S. W. & Wichmann, J. Breaking the diffraction resolution limit by stimulated emission: stimulated-emission-depletion fluorescence microscopy. *Opt. Lett.* **19**, 780–782 (1994).

181. Dyba, M. & Hell, S. W. Focal Spots of Size λ / 23 Open Up Far-Field Florescence Microscopy at 33 nm Axial Resolution. *Phys. Rev. Lett.* **88**, (2002).

182. Hess, S. T., Girirajan, T. P. K. & Mason, M. D. Ultra-High Resolution Imaging by Fluorescence Photoactivation Localization Microscopy. *Biophys. J.* **91**, 4258–4272 (2006).

183. Rust, M. J., Bates, M. & Zhuang, X. Sub-diffraction-limit imaging by stochastic optical reconstruction microscopy (STORM). *Nat. Methods* **3**, 793–796 (2006).

184. Jones, S. A., Shim, S.-H., He, J. & Zhuang, X. Fast, three-dimensional super-resolution imaging of live cells. *Nat. Methods* **8**, 499–505 (2011).

185. Heilemann, M. *et al.* Subdiffraction-Resolution Fluorescence Imaging with Conventional Fluorescent Probes. *Angew. Chem. Int. Ed.* **47**, 6172–6176 (2008).

186. Heine, J. *et al.* Adaptive-illumination STED nanoscopy. *Proc. Natl. Acad. Sci.* **114**, 9797–9802 (2017).

187. Klar, T. A., Jakobs, S., Dyba, M., Egner, A. & Hell, S. W. Fluorescence microscopy with diffraction resolution barrier broken by stimulated emission. *Proc. Natl. Acad. Sci.* **97**, 8206–8210 (2000).

188. Gustafsson, M. G. L. *et al.* Three-Dimensional Resolution Doubling in Wide-Field Fluorescence Microscopy by Structured Illumination. *Biophys. J.* **94**, 4957–4970 (2008).

189. Huang, B., Wang, W., Bates, M. & Zhuang, X. Three-Dimensional Super-Resolution Imaging by Stochastic Optical Reconstruction Microscopy. *Science* **319**, 810–813 (2008).

190. York, A. G., Ghitani, A., Vaziri, A., Davidson, M. W. & Shroff, H. Confined activation and subdiffractive localization enables whole-cell PALM with genetically expressed probes. *Nat. Methods* **8**, 327–333 (2011).

191. Lin, C. *et al.* Submicrometre geometrically encoded fluorescent barcodes self-assembled from DNA. *Nat. Chem.* **4**, 832–839 (2012).

Box 1: SRM basics

Structured illumination microscopy (SIM). SIM relies on the illumination of the sample using high-spatial frequency patterns [176]. Basically, the excitation light is not homogenous but has a specific profile, typically parallel lines as shown in Fig.1. When a sample containing features smaller than the diffraction limit is illuminated, the combination of the patterned illumination and the sample generates large detectable interference patterns (Moiré fringes). The incident pattern is typically applied in different orientations and, as the illumination profile is known, a super resolution image can be mathematically deconvolved from the interference signal. This approach leads to a lateral resolution of about 125 nm and an axial resolution of about 350 nm. Moreover, sub-second temporal resolution can be obtained without the necessity of high illumination powers making SIM suitable for live-cell imaging[177]. More

advanced approaches such as non-linear SIM[178] and instant SIM (iSIM) [179] allow us to reach spatial and temporal resolution down to 50 nm and 30 ms, respectively.

Stimulated emission depletion (STED). STED achieve super-resolution by reducing the size of the effective point spread function, i.e. the excitation volume. [180]. This is achieved by illuminating the sample with two aligned beams: a classical confocal excitation beam (to excite fluorescence) and a doughnut-shaped beam (that rapidly turns-off the emission by means of stimulated emission)as shown in Fig.1. Basically, only the fluorophores close to the center of the doughnut will emit resulting in a reduced PSF and therefore improved resolution. Typically, STED can reach a lateral resolution of 50-80 nm with a temporal resolution of seconds, comparable to a confocal microscope. Depending on the samples, higher resolution can be obtained. In particular interferometric approaches such as 4Pi allowed to improve the axial resolution down to 40 nm [181].

Single molecule localization microscopy (SMLM). SMLM achieves sub-diffraction resolution with the accurate localization of individual fluorophores under a wide field illumination [150,182,183]. In these methods, the dye emission is photocontrolled, and the fluorophores can be swithched on/off with laser illumination. This is used to have the large majority of the dyes in the off state and only a few sparsely distributed dyes are emitting. Thanks to this the fluorescence of single markers can detected and the precise spatial positioning of the emitting molecules can be identified by fitting a Gaussian profile and obtaining the Gaussian centroid. This operation is iterated and for every frame few tens of molecules are identified until all the dyes in the sample are localized. By summing up the position of all molecule detected a super resolution image is obtained. Therefore, depending on the photons detected a resolution of 20-25 nm can be routinely achieved and more advanced setups enabled a resolution of 5 nm [76] at the price of a lower temporal resolution (typically minutes) and more cumbersome sample preparation (for example, involving the use of special fluorophores and buffers). Moreover, novel approaches to improve temporal resolution down toseconds have been reported [184]. The most used SMLM methods are photoactivated localization microscopy (PALM) [150], (direct) dtochastic optical reconstruction microscopy ((d)STORM) [183,185] and points accumulation for imaging in nanoscale topography (PAINT) [12]. These methods are all based on the same experimental imaging setup and differ mostly in the way a small subset of single molecules is activated.

Box 2. How to choose the most suitable SRM method for synthetic samples

The different super resolution microscopy (SRM) techniques present different advantages and disadvantages, it is therefore crucial to choose the ideal technique to answer the desired scientific question.

Single molecule localization microscopy (SMLM) methods are endowed with the best spatial resolution (typically 20 nm, down to 5 nm in special cases), single molecule sensitivity and potentially enable quantitative molecular counting. However, their poor temporal resolution doe hampers live-cell imaging. SMLM also requires the use of special probes (photoswitchable dyes) and experimental conditions (special buffer containing mixture of redox reagents). Therefore, this approach is preferred for static measurements for which the maximum resolution is needed and when information at the single molecule level is desired. Moreover, a high density of labels is necessary to achieve the optimal resolution and this can result in a perturbation of the structure of interest. This is particularly true when small molecules need to be labeled (for example, small molecular building blocks for self-assembly), as the dye structure may largely affect the molecular properties. Therefore, special care has to be taken in the experimental design and sample preparation.

Structured illumination microscopy (SIM), on the contrary, enables easy and reasonably fast imaging with standard fluorophores. SIM approaches are recommended when the sample preparation and labeling are particularly challenging. Moreover, SIM does requires less illumination power than SMLM and STED and it is therefore suggested for photosensitive samples. However, the resolution of SIM (typically 120 nm) is significantly worse than SMLM and STED and therefore can be useful to iamge materials morphology but cannot answer questions on the molecular scale.

Finally, Stimulated emission depletion (STED) provides an intermediate spatial and temporal resolution and less limitations than SMLM in the sample preparation. For these reasons, it is commonly used for the study of synthetic samples that do not need extreme

resolution and single molecule sensitivity. Notably, the high power required for STED can be an issue for synthetic samples that are not photochemically or thermally stable and controls for photodamage would be needed. Notably STED can be easily coupled with other methods such as time resolved and wavelength-resolved microscopies [186], *for example* STED / fluorescence correlation spectroscopy.

Figures

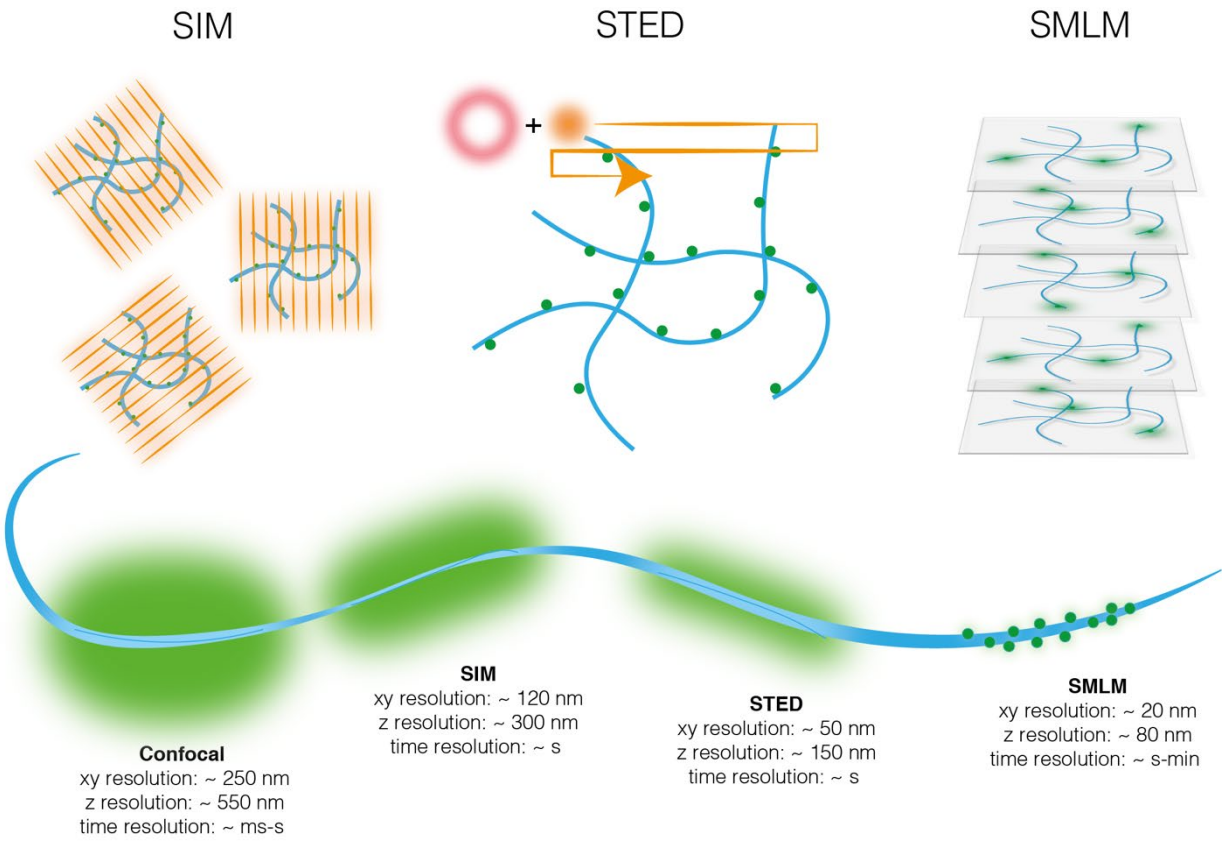

Fig.1 - Schematic representations of image acquisition procedure for the three main families of super resolution microscopy techniques. The typically attainable lateral (xy), axial (z) and time resolutions are indicated[187–190]. These values may change according to the wavelength, type of sample and experimental setup employed. See BOX 1 for more detailed technical information.

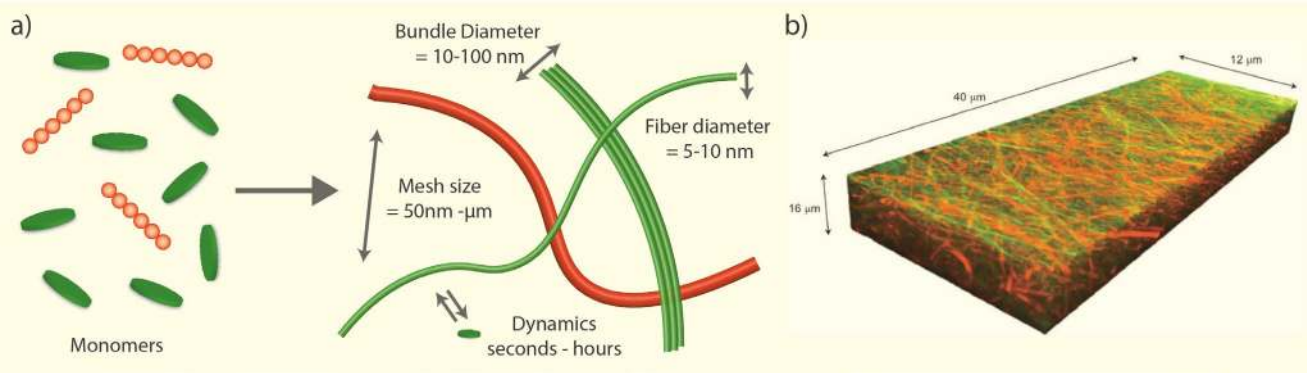

Figure 2. a) Schematic representation of the structural and functional properties of self-assembled supramolecular polymers. Momers, typicall small amphiphilic molecules, after injection in the solvent of interest can self-assemblt into fibrillar structures. This can be stable as isolated fibers in solution, they can bundle forming higher-hierarchy materials or, typically at high concentration, form hydrogels. Several structural features are therefore crucial to be imaged: the fiber length and diameter, their bundling and the 3D features of gels such as the mesh size. **b)** STED imaging of supramolecular hydrogels, adapted with permission from REF[28].

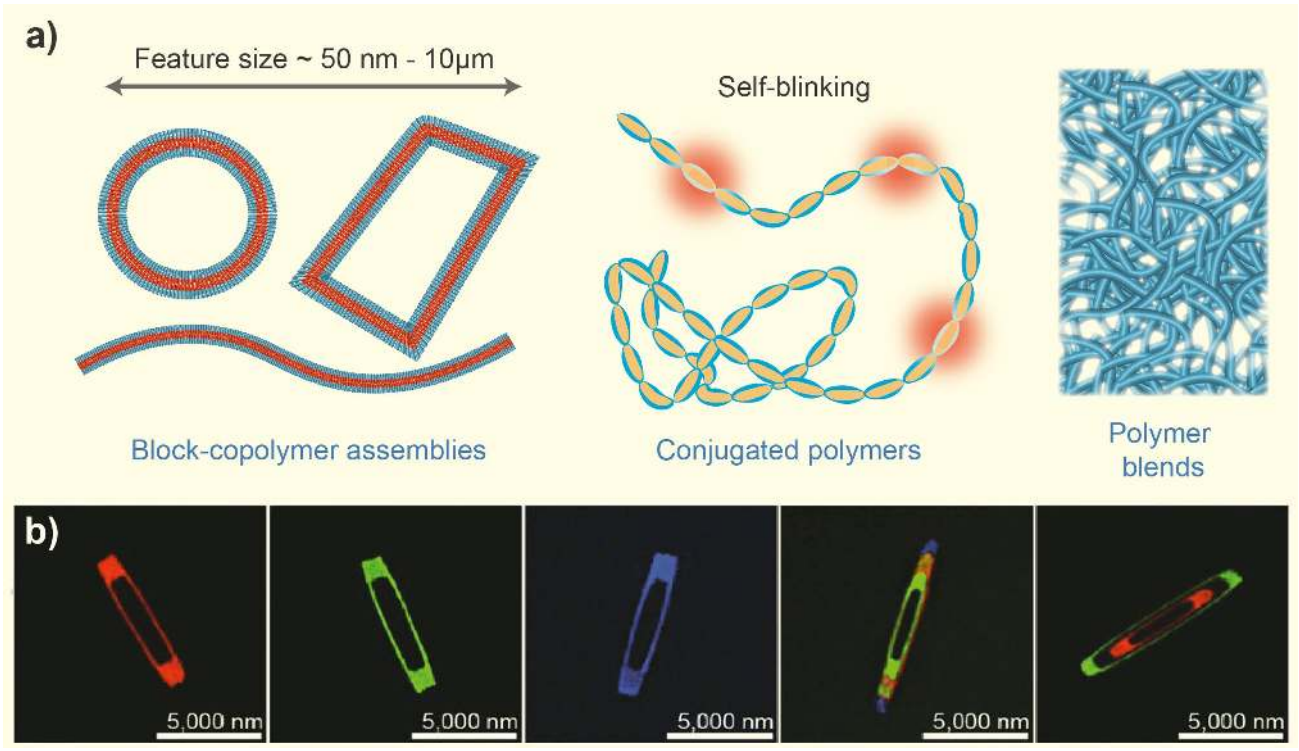

Fig.3 – a) Schematic representations of the main families of polymeric materials studied with SRM: block-copolymer assemblies, conjugated polymers and polymer blends. Together with structural features such as length, diameter and morphology super resolution microscopy can help to probe functional features such as the self-blinking of conjugated polymers, a key features for their electronic behaviour. **b)** SIM imaging of platelet-like block-copolymer micelles, adapted with permission from REF [31].

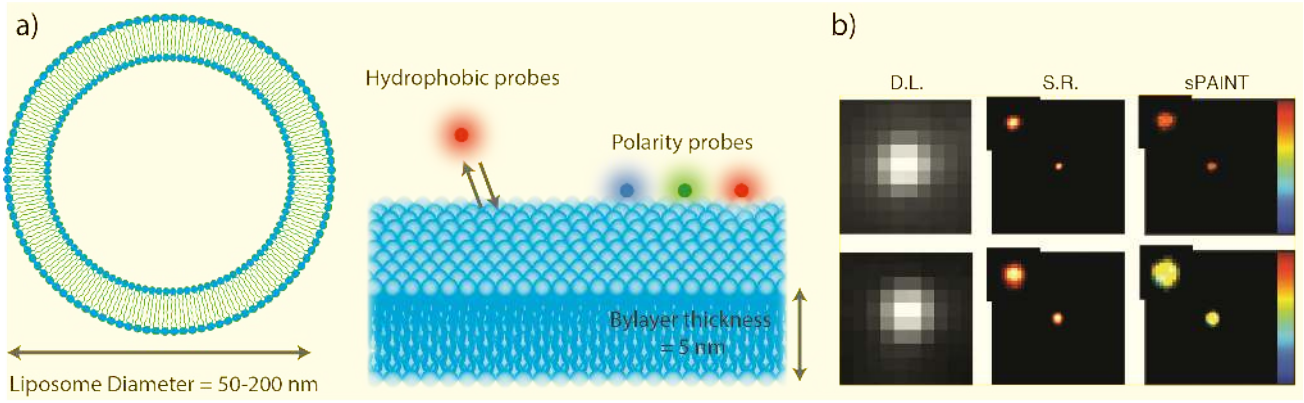

Fig.4 – a) Schematic representations of the structures and features of lipid materials: liposomes (left) and supported lipid bylayers (middle). Together with their size and morphology super-resolution microscopy can probe the material polarity using solvatochromic probes, a key aspect of lipid-based materials. **b)** Study of lipid assemblies using spectral-PAINT, adapted with permission from REF [57], revealing liposomes nanostructure and polarity.

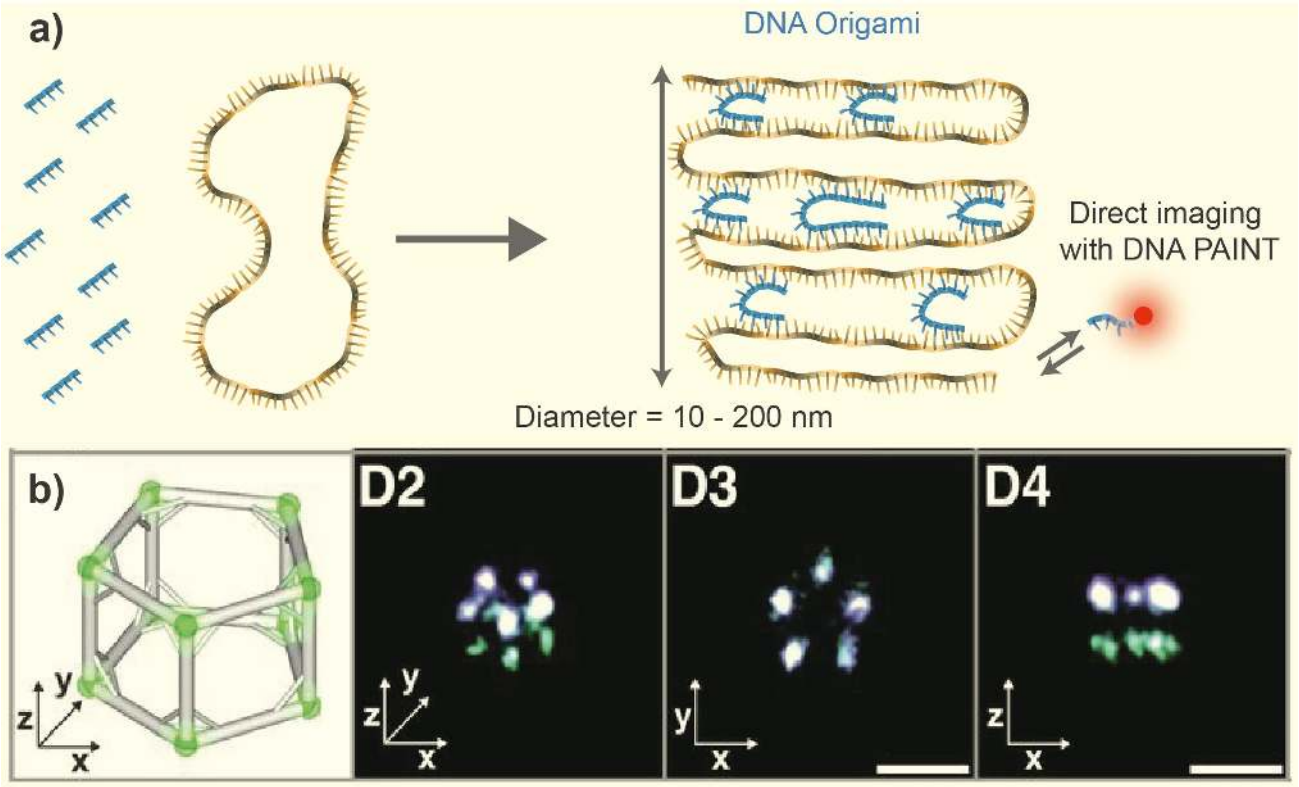

Fig.5 – a) Schematic representations DNA origami structure and features. DNA Origami self-assemble from multiple DNA strands through programmed DNA-DNA hybridization. Due to the intrinsic composition of DNA origami DNA-PAINT is the most used super-resolution technique to characterize these structures. Indeed, in this method small dye-labeled DNA strands can be used to directly probe the origami structure by reversible and specific hybridization. **b)** 3D-PAINT imaging of DNA origami, adapted with permission from REF [191]

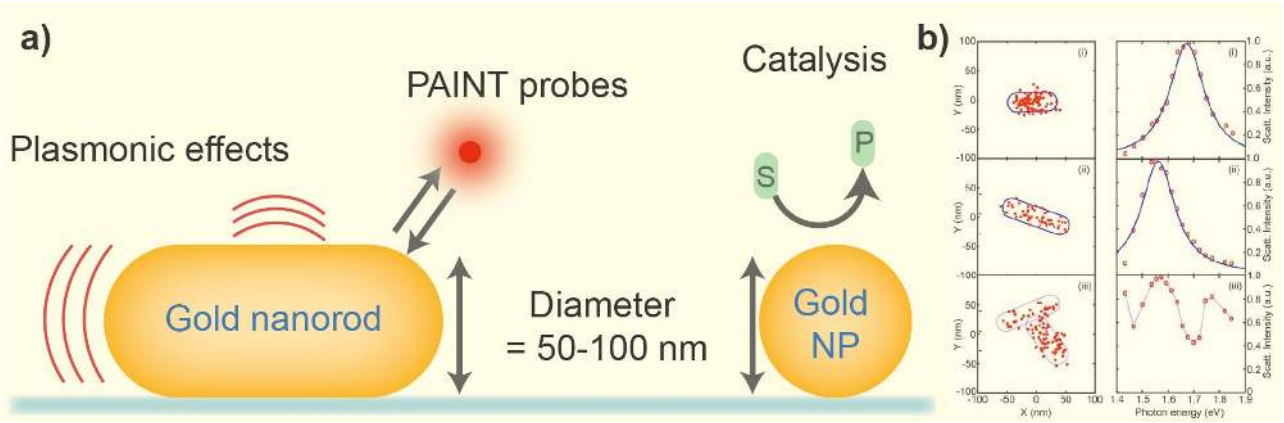

Fig.6 – a) Schematic representations of the structural and functional features of metal NPs. In particular gold nanorods and nanoparticles are extensively used to their intrinsic properties such as plasmonic effects and catalytic activity. SRM has been used to probe both of these unique features as they both can interphere with fluorescence emission. In this framework SRM can not only provide structural information (e.g. particle size and morphology) but also functional information on NPs plasmonic and catalytic activity. **b)** DNA-PAINT imaging of AuNPs, adapted with permission from REF [103]

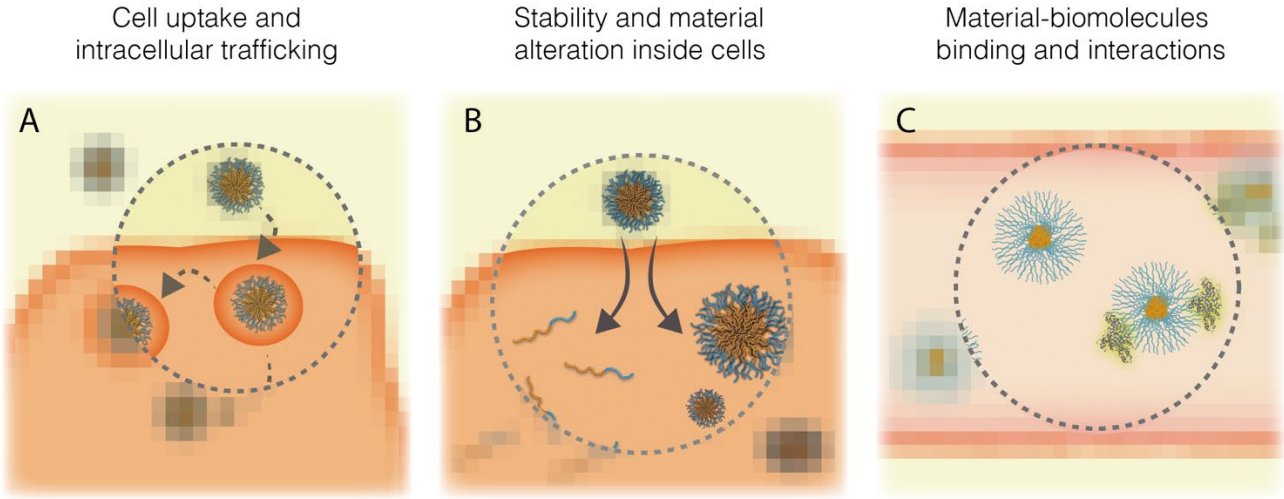

Figure 7. Interactions between materials and cells or biomolecules can be studied with nanometric resolution using super-resolution microscopy. a) The cell uptake and the exact intracellular localizations can be studied providing nanometric information which can be relevant for the material application. All SRM methods are used to study intracellular localization of NPs in fixed cells (SMLM, STED) and live cells (SIM, STED). **b)** The structure and the stability of the material internalized can be studied using SRM providing information about changes on the materials at the nanometric scale. Both SIM and SMLM are used to probe shape and size changes following cell uptake. **c)** Materials once introduced into living systems can interact with an enormous number of biomolecules. To design effective materials, it is important to understand the binding and the interactions with these biomolecules, which can affect their functionality. 2-color SMLM is used to measure bio-nano-interactions at the single molecule level.

GLOSSARY:

Abbe's criteria: states the resolution theoretically obtainable considering the diffraction of light. Ernst Abbe described in 1873 that using light of a wavelength λ, traveling through a medium of refractive index n focused with a half-angle θ the minimum resolution possible is $\lambda/2n\sin\theta$

far-field optical techniques: optical microscopes that use configurations where light does not pass through sub-wavelength features.

4Pi microscopy: is a fluorescence microscope that achieve an improved axial resolution using two objective lenses focused to the same spatial location

Recombinant proteins: translated products of the expression of recombinant DNA non-native to the living cells (e.g., bacteria, mamallian, yeast) used for the expression

stepwise photobleaching: is the sequential loss of fluroscence of individual molecules resulting in a series of distinguishable steps that provide information about the number of fluorophores present.

transmission diffraction grating: is a device with a periodic structure that diffracts incident light into different components by wavelength.

protein corona: is the layer of adsorbed protein on the surface of a nanoparticle exposed to biological fluids like blood. It can be divided in hard corona, the stabily-bound proteins, and soft corona, the loosely and reversibly bound proteins.